

STRESS DISTRIBUTION IN THE END BLOCK OF A  
POST-TENSIONED PRESTRESSED CONCRETE BEAM

Thesis for the Degree of M. S.  
MICHIGAN STATE UNIVERSITY  
Piyush Chandra Sharma  
1961

**This is to certify that the**

**thesis entitled**

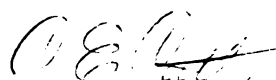
**"Stress Distribution in the End Block of a  
Post-Tensioned Prestressed Concrete Beam"**

**presented by**

**Piyush Chandra Sharma**

**has been accepted towards fulfillment  
of the requirements for**

**M.S degree in Civil Engineering**



**Major professor**

**Date** Nov 1, 1961

STRESS DISTRIBUTION IN THE END BLOCK  
OF A POST-TENSIONED PRESTRESSED  
CONCRETE BEAM

By

Piyush Chandra Sharma

A THESIS

Submitted to  
Michigan State University  
in partial fulfillment of the requirements  
for the degree of

MASTER OF SCIENCE

Department of Civil Engineering

1961



## ACKNOWLEDGEMENTS

The author wishes to express his sincere appreciation and thanks to his major professor, Dr. C. E. Cutts, for his inspiration and guidance throughout this investigation. He is also indebted to Dr. W. A. Bradley for his keen interest and invaluable help.

The writer wishes to express thanks to Mr. H. A. Elleby for his help in the computer work and experimental investigation.

The author wishes to express his gratitude to the T.C. M. and I. C. A. (International Cooperation Administration) for their sponsorship, which made this work possible.

## ABSTRACT

# STRESS DISTRIBUTION IN THE END BLOCK OF A POST-TENSIONED PRESTRESSED CONCRETE BEAM

By Piyush Chandra Sharma

The object of this study is to investigate the distribution of stress in the end block of a post-tensioned prestressed concrete beam. The beam has been considered a two-dimensional elasticity problem in plane stress with the stresses perpendicular to the plane of the beam equal to zero. The technique utilizing Airy's Stress functions was applied and the resulting differential equations were solved by the finite difference method on the "Mistic" digital computer.

In order to check the theory, experimental measurements were made on the end block of a post-tensioned prestressed concrete beam. SR-4 Rosette Electrical Strain Gages were placed in a grid at the end of the member and strains were measured for a ten ton tensile load in the cable. While the laboratory experiments did not exactly duplicate the theoretical solution in dimensions of beam and bearing plate detail, it did afford a good comparison of conditions and variations of stress in an end block.

It was found that the experimental variation of stresses agreed well with the theoretical solution. In magnitude also there was good agreement except for the shearing stresses, which were too small in both the cases to have any considerable effect on others.

## INDEX

INTRODUCTION . . . . .	1
REVIEW OF PREVIOUS INVESTIGATION. . . . .	3
SCOPE OF INVESTIGATION. . . . .	32
THEORETICAL INVESTIGATION . . . . .	34
EXPERIMENTAL INVESTIGATION. . . . .	59
DISCUSSION. . . . .	67
CONCLUSIONS . . . . .	70
BIBLIOGRAPHY . . . . .	71

## I INTRODUCTION

Whenever a concentrated load or pressure acting over a limited area is applied to the ends of a beam, the stresses at some distance from the point of application of the load vary linearly over the cross section and are statically determinate but the stress distribution near the load is no longer linear and is statically indeterminate.

This follows from the principle of Saint Venant which states that if the forces acting on a small portion of the surface of an elastic body are replaced by another statically equivalent system of forces acting on the same portion of the surface, this redistribution of loading produces substantial changes in the stresses locally, but has a negligible effect on the stresses at distances which are large in comparison with the linear dimensions of the surface on which the forces are changed.

In post-tensioned prestressed concrete beams the prestressing force is applied at the ends of the beam over a comparatively small area of the cross section. This force is transmitted through a steel bearing plate, which is assumed to produce a uniform pressure at the ends. This distribution tends to be uniform as the thickness of the bearing plate is increased and decreases with the plate action. In general, the distribution is assumed to be uniform beneath the bearing plate .

This uniform pressure applied over a small area becomes either a uniformly varying pressure or a constant pressure at some distance from

the bearing plate, depending upon the position of the resultant force on the end of the beam.

In this study, the resultant force has been assumed to act at the middle third of the beam section and the experimental beam likewise fulfills this condition.

The purpose of this study is two-fold. First, to investigate analytically the distribution of stress near the ends of the beam (namely in the end block) by means of the theory of elasticity. Secondly to compare experimental measurements taken in the laboratory with the analytical solution.

## II REVIEW OF PREVIOUS INVESTIGATION

The distribution of stress caused by a concentrated load acting upon a large mass was originally worked out by Boussinesq (1885) in which he developed relationships for stress variation in a semi-infinite solid. These relationships have been used in determining stresses in soil masses due to surcharge forces for both point and uniform type loadings.

A closely related problem is the transmittal of the concentrated load in a column to the supporting footing. An experimental investigation by Richart (19) at the University of Illinois (1932) showed that in practically all the cases stresses in the footing were distributed uniformly at an angle of  $45^{\circ}$  with the edge of the bearing plate.

J. N. Goodier (9), (1932) analyzed the problem of stress distribution in a plate due to concentrated loads, using the Theory of Elasticity. The stress distribution was solved for blocks with varying dimensions. He considered the case of a rectangular plate or block compressed by knife edge loadings at the top and bottom of the block. It was shown that tensions of considerable magnitude developed across the middle plane through the knife edges. These tensions vary with the distribution of the load over the bearing area. (fig. 1).

With the increasing use of prestressed concrete, greater attention has been focused on this problem and a number of theoretical treatments

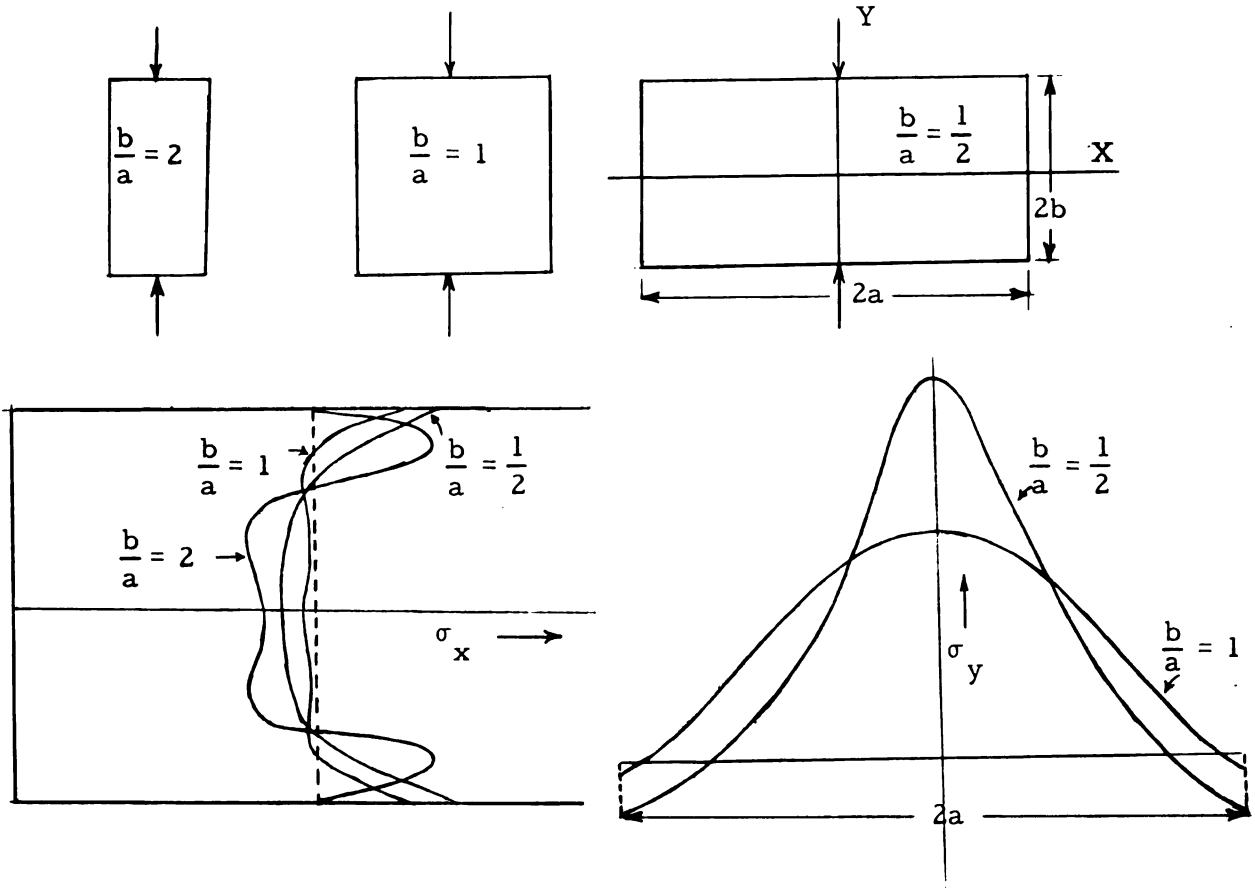


Fig. 1. Variation of stresses according to Goodier's analysis

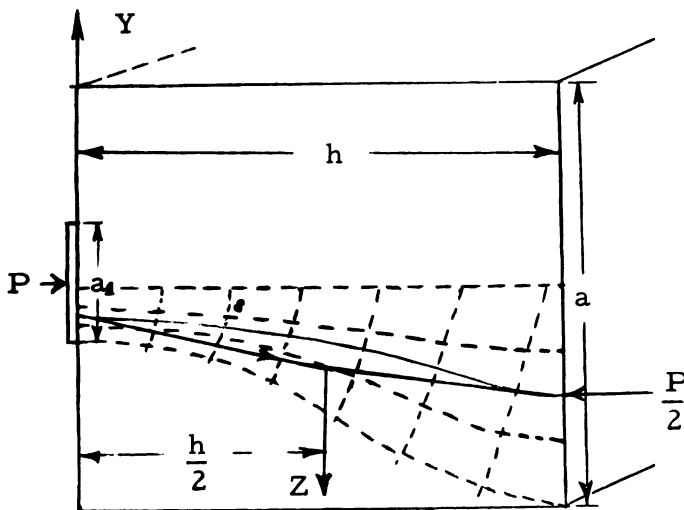


Fig. 2a. Stress trajectories in Mörsch theory

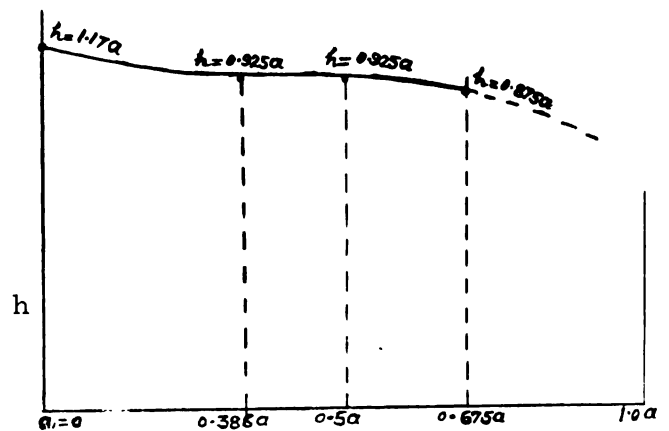


Fig. 2b. Relation between h and a

have been developed. Since some of the theories have been recommended for the design of end blocks in prestressed concrete units, or have been used as the basis for study of stress distribution in the end block, they warrant special attention.

### Mörsch's Theory

The first approach to the calculation of stresses in blocks subjected to concentrated loads was developed by Mörsch (17) in 1924. It is based on the following assumptions:

(1) The stresses due to a concentrated load are uniformly distributed at a distance equal to the width of the prism.

(2) The curvature of trajectories causes the tensile stresses, the latter being distributed according to a parabolic variation.

The last assumption was justified by Mörsch on the basis of Krüger's measurements of transverse strain (Deutsche Bauzeitung, 1906, Paper 263) but Krüger measured the strains only at three points from which he constructed a parabola representing the stress distribution.

The distribution of compressive stress trajectories deduced by Mörsch is shown in fig. 2a if the compressive stresses are uniform over both the loaded area and the remote end of the end block. Then the force  $Z = \frac{p(a - a_1)}{4h}$  and hence the maximum tensile stress for a rectangular prism of breadth  $b$  is

$$\sigma_y = \frac{3Z}{2ab}$$

Mörsch carried out tests mainly on stone blocks, however, a few tests were conducted with concrete blocks. He applied a correction to the depth of block ( $h$ ) as shown in fig. 2b to bring the tensile stresses at cracking load according to the above formula and the actual tensile strength of the material of which the block is made, in agreement. During the tests Mörsch discovered that there was no visible influence of reinforcement on the cracking and ultimate load of the blocks and he suggested that it was more important to use high strength concrete, than to employ large amounts of reinforcement for the blocks.

### Bortsch's Theory

One of the theoretical approaches to the problem of bearing capacity as well as stress distribution in structural units under concentrated loads is due to Bortsch (3, 4), (1935). He considered a hinge block as a deep beam of infinite length subjected to a load distributed on the contact area in the form of a cosine function (fig. 3). The amplitude of the cosine function is  $p_1 = \frac{\pi P}{2a_1}$ , following equations were derived

$$\sigma_y = -\frac{2P}{a} \sum_{n=1,3,5}^{\infty} \left(1 - \frac{n\pi x}{a}\right) e^{\frac{n\pi x}{a}} \left\{ \left(1 - \frac{n^2 \beta^2}{n^2 \beta^2 - 1}\right) \cos \frac{n\pi \beta}{2} \right. \\ \left. + (-1)^{\frac{n+1}{2}} \frac{2}{n\pi} \right\} \cos \frac{n\pi y}{a}$$

$$\sigma_x = -\frac{2P}{a} \sum_{n=1,3,5}^{\infty} \left(1 + \frac{n\pi x}{a}\right) e^{-\frac{n\pi x}{a}} \left\{ \left(1 - \frac{n^2 \beta^2}{n^2 \beta^2 - 1}\right) \cos \frac{n\pi \beta}{2} \right.$$

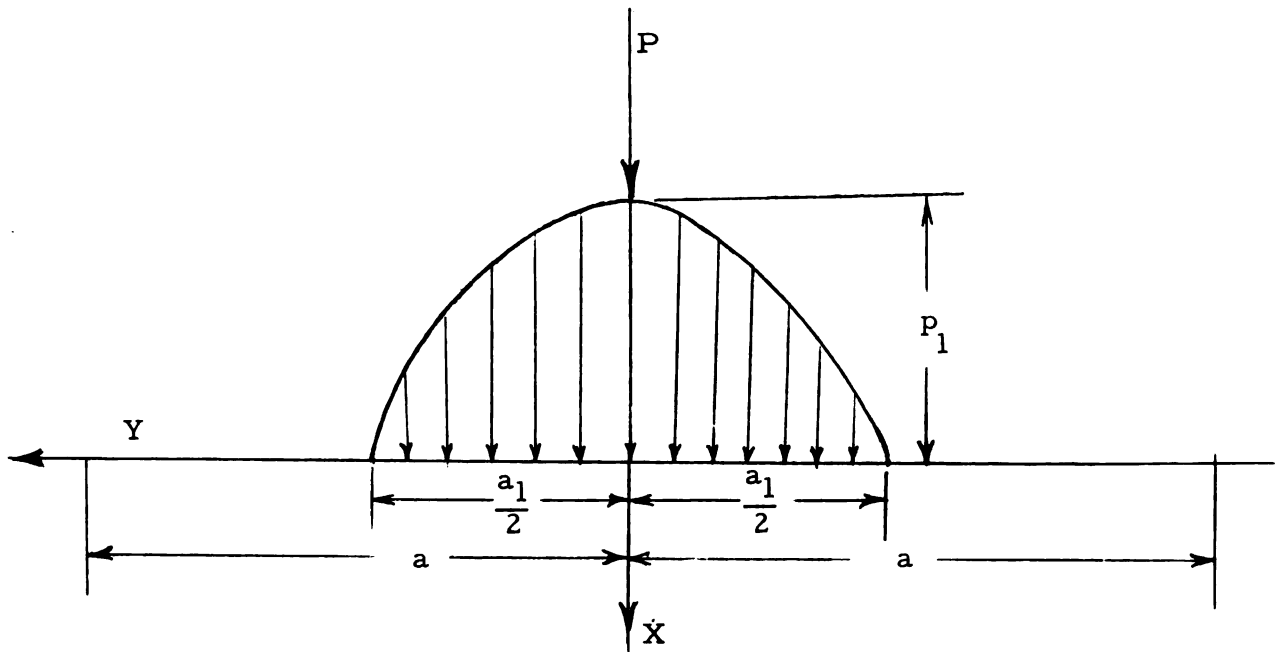


Fig. 3. Load distribution in Bortsch theory

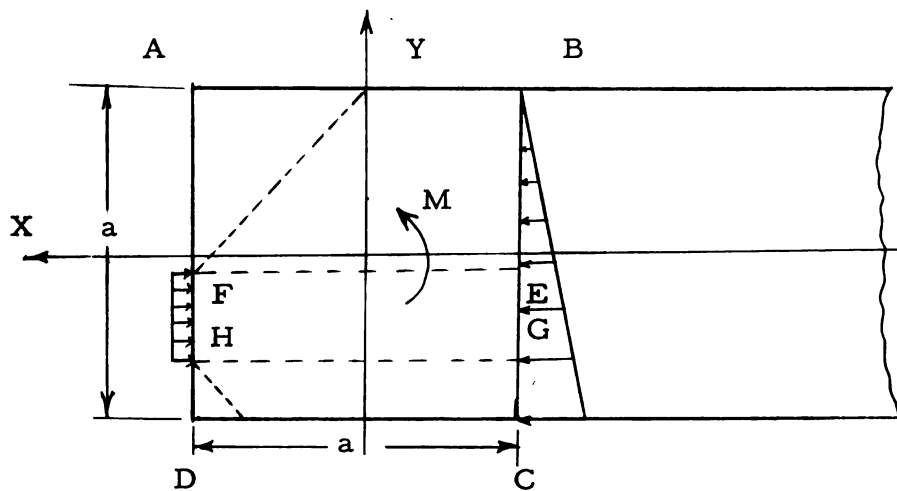


Fig. 4. End block in Magnel's theory

$$\tau_{xy} = +\frac{2P}{a} \sum_{n=1,3,5}^{\infty} \frac{n\pi x}{a} e^{-\frac{n\pi x}{a}} \left\{ \left(1 - \frac{n^2 \beta^2}{2\beta^2 - 1}\right) \cos \frac{n\pi y}{2} + (-1)^{\frac{n+1}{2}} \frac{2}{n\pi} \right\} \cos \frac{n\pi y}{a}$$

$$+ (-1)^{\frac{n+1}{2}} \frac{2}{n\pi} \left. \right\} \sin \frac{n\pi y}{a}$$

The stresses can be evaluated for various values of  $\beta = \frac{a_1}{a}$  ratio for any point given by the values  $x/a$  and  $y/a$ . Maximum transverse tensile stresses occur on the central axis of the block, at distance between the end of the block given by  $x/a = .2$  to  $.3$  and the magnitude of maximum tensile forces being  $.38$  to  $.45 \frac{P}{a}$  for  $\beta = .2$  and  $.1$ . At a distance of  $x/a = 1.7$  from the end the tensile forces are almost negligible.

Bortsch dealt with small values of  $\beta$  ranging from  $0$  to  $.2$  and did not indicate whether his theory could be used for  $\beta$  approaching unity, as occurs in most cases in the anchorage zone of post-tensioned members. Tests carried out by Jesinghams (3) confirm to some extent the general shape of the Bortsch curve for the  $\sigma_y$  stresses, showing that the cracks in the block developed close to the central axis. The recent tests by Kammüller (13) give the abscissa of maximum tensile stress as  $x/a = .22$  which agrees satisfactorily with Bortsch's theory, but differs from Mörsch theory.

### Magnel's Theory

The first analysis dealing directly with this problem of end block analysis was proposed by Professor Gustav Magnel (14) in his text published in 1948. The author suggested an approximate method of computing the stresses in a prestressed beam end block.

This method consisted of considering the end block as a free body. The stress distribution at a distance equal to the depth is considered to vary linearly and is given by the classical formula

$$\sigma = \frac{P}{A} + \frac{My}{I}$$

Block ABCD was analyzed for stresses caused by the loading shown there will be bending and shearing stresses induced perpendicular to and along the planes FE, HG and other similar planes. Shear stress can be calculated by using the formula  $\tau = \frac{VQ}{Ib}$ . (fig. 4).

Similarly, bending stresses were calculated by considering ABEF and GHDC as cantilevered sections with the load causing bending being the triangular load on section BC. The stress  $\sigma_x$  in the longitudinal direction was evaluated by assuming the pressure dispersion takes place at an angle of approximately  $45^\circ$ .

In the same text, Professor Magnel proposes a second theory in which stresses due to bending perpendicular to a plane parallel with the longitudinal axis of the beam vary as a second degree parabola.

$$\sigma_y = \frac{12M}{bD^2} \left[ -1 + \frac{4x}{D} - \frac{3x^2}{D^2} \right]$$

where

M = moment

b = width

D = depth

x = distance in the direction from a reference point located at  $1/2D$ .

This gives a maximum compressive stress of  $\frac{12M}{bD^2}$  and a maximum tensile stress of  $\frac{4M}{bD^2}$ .

In the second edition of Professor Magnel's (15) book published in 1950, this theory was modified. Instead of considering the stress as varying as the second degree parabola, it was modified to vary as a third degree parabola.

Magnel assumed that the stresses under the bearing plate dispersed at an angle of 45 degrees into the end of the beam and that at each plane 1-1, 2-2 etc., the ordinary laws of eccentric compression apply. The typical distribution of pressure on planes 1-1, and 2-2 is shown in fig. 5.

In all cases, only the effective width is used in computing the area and moment of inertia, for areas outside the 45 degree dispersion line the vertical stress is zero. As described before, by considering the element ABCD as a force body, the loading causes a shear S and a moment M on any vertical plane EF, GH etc.

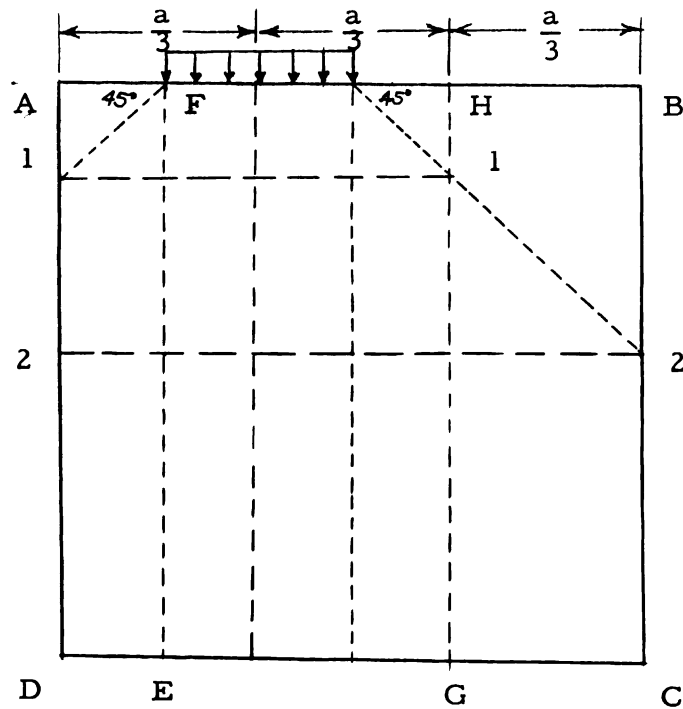


Fig. 5. Dispersion of load in Magnel's theory

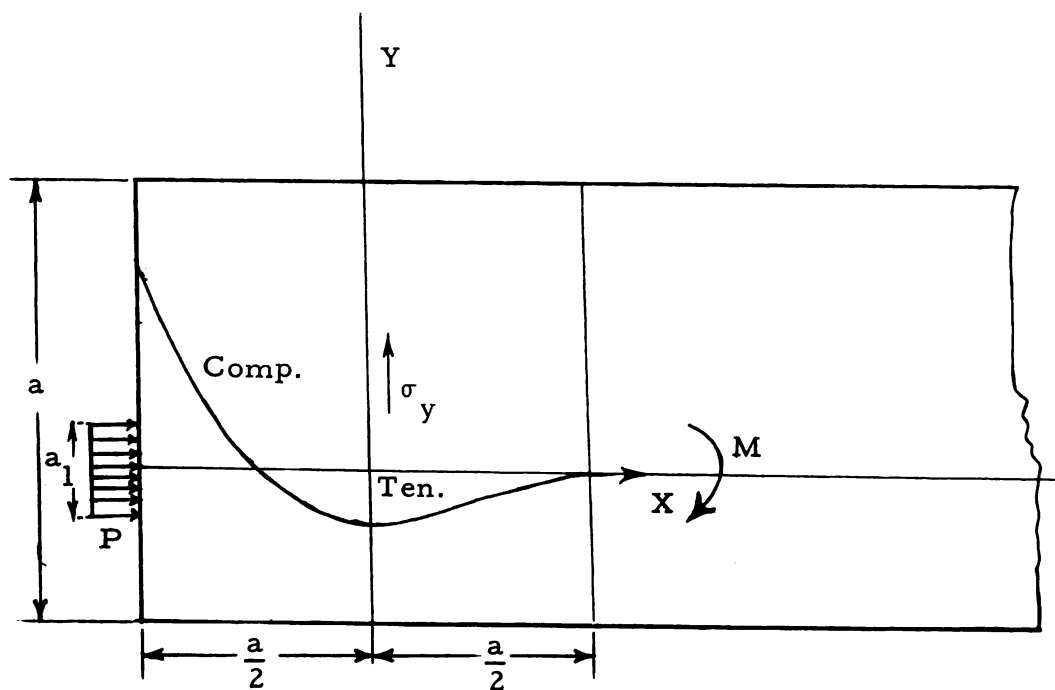


Fig. 6. End block and transverse stress distribution in Magnel's theory

The  $\sigma_y$  stresses produced due to M on any of the vertical sections have a stress distribution diagram in the form of a third degree parabola (fig. 6).

The general equation of the cubic parabola is  $\sigma_y = A + Bx + Cx^2 + Dx^3$ .

Where A, B, C and D are unknown coefficients to be evaluated by applying four different conditions. These four limiting conditions are

$$(1) \quad \text{At } x = -\frac{a}{2}; \quad \sigma_y = 0$$

$$(2) \quad \text{At } x = -\frac{a}{2}; \quad \frac{d\sigma_y}{dx} = 0$$

(3) Sum of the forces in the y direction must equal zero.

$$\int_{-\frac{a}{2}}^{\frac{a}{2}} \sigma_y \cdot b \, dx = 0$$

where b = width of beam.

(4) On any plane EF or GH etc.

$$M = \int_{-\frac{a}{2}}^{\frac{a}{2}} \sigma_y \cdot x \cdot b \, dx$$

Substituting these conditions the values of A, B, C and D are obtained.

$$A = \frac{-5M}{2ab}, \quad B = 0, \quad C = \frac{60M}{4ab} \quad \text{and} \quad D = \frac{80M}{5ab} \quad \text{then}$$

$$\sigma_y = \frac{5M}{ba} \left[ -1 + \frac{12x^2}{a} + \frac{16x^3}{3a} \right] = K \frac{M}{a^2 b} \quad \text{where K is a coefficient.}$$

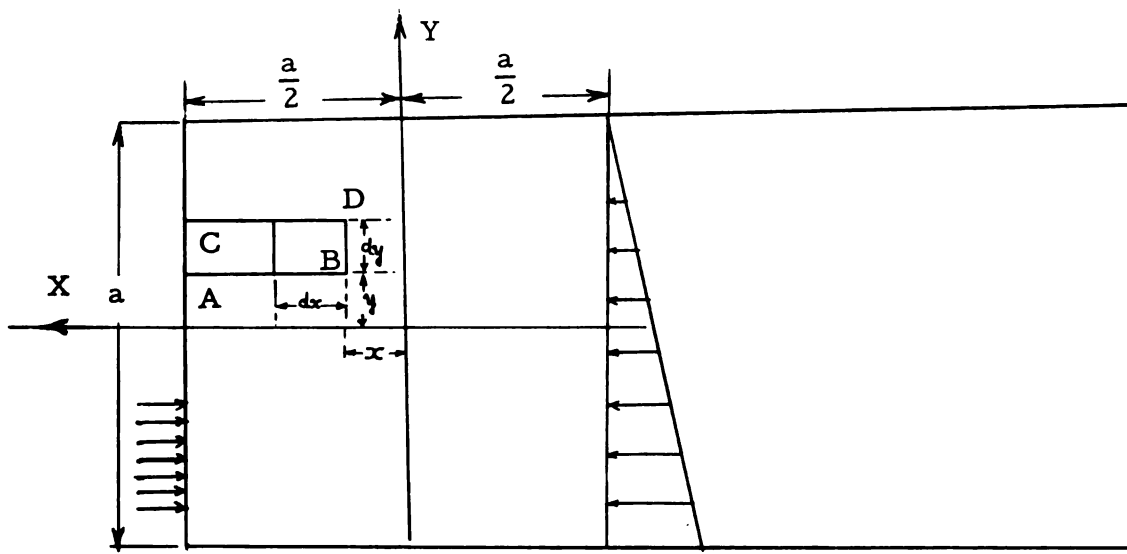


Fig. 7. End block showing the movement of section for computing the shearing stresses by Magnel's method

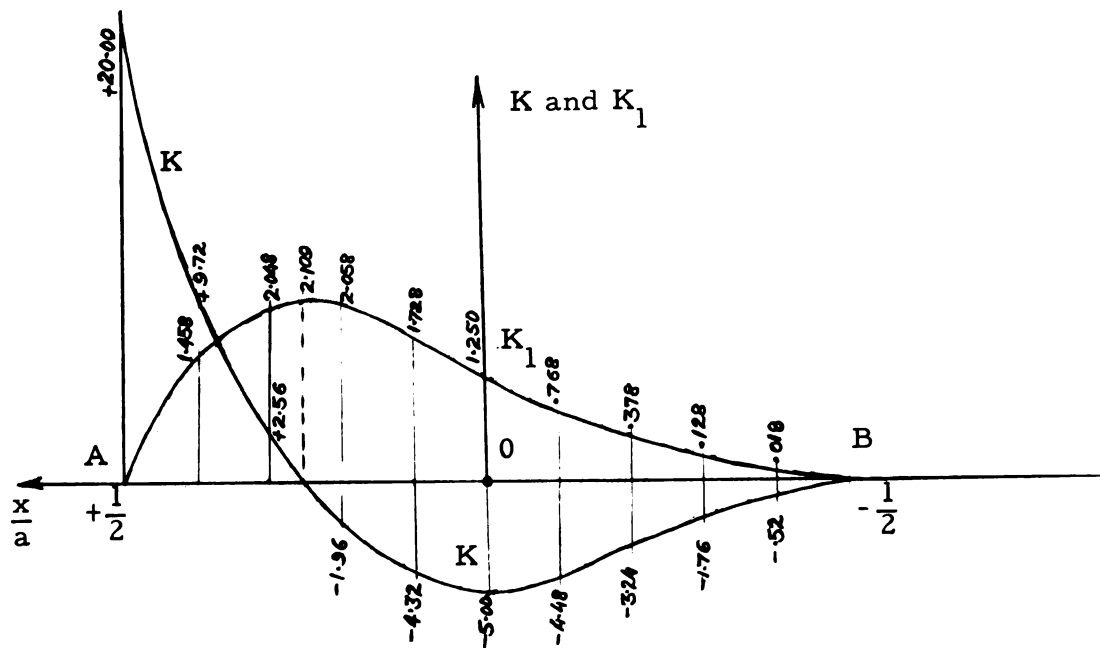


Fig. 8. Value of  $K$  and  $K_1$  in Magnel's theory

When the law of variation of  $\sigma_y$  stresses is known, the shearing stresses  $\tau_{xy}$  can be evaluated. Consider a slice of concrete between  $\frac{a}{2} > x > 0$  and  $\frac{a}{2}$  and two parallel planes having an ordinate of  $y$  and  $y + dy$  is isolated (fig. 7). This slice of concrete is subjected to a bending moment  $M$  on the  $y$  plane and another bending moment  $M + dM$  on the  $y + dy$  plane. The unbalanced  $\sigma_y$  force produced by these bending moments is resisted by shear on plane DB.

The change in force between the planes  $y$  and  $y + dy$  becomes

$$\frac{d\sigma_y}{dy} dy$$

Total force on plane AB thus equals

$$\int_{-\frac{a}{2}}^{\frac{a}{2}} \frac{d\sigma_y}{dy} dy$$

considering unit width of beam. For equilibrium

$$\tau_{xy}(dy) = \int_x^{\frac{a}{2}} \frac{d\sigma_y}{dy} dy dx$$

also  $\frac{d\sigma_y}{dy} = \frac{k}{ba^2} \frac{dM}{dy}$ ; since  $\sigma_y = \frac{KM}{ba^2}$ . Now  $\frac{dM}{dy} = \text{shear } S$ , therefore

$$\frac{d\sigma_y}{dy} = \frac{K}{ba^2} S \text{ and } \tau_{xy} = \int_x^{\frac{a}{2}} \frac{k}{ba^2} \cdot S \cdot dx = \frac{s}{ba^2} \int_x^{\frac{a}{2}} K dx.$$

$$K = S \left[ \left( -1 + \frac{12x^2}{a^2} \right) x - \frac{16x^3}{a^3} \right]_{x}^{\frac{a}{2}}. \text{ Therefore } \tau_{xy} = \frac{5S}{ba} \left[ \frac{1}{4} + \frac{x}{a} - \frac{4x^3}{a^3} - \frac{4x^4}{a^4} \right] \text{ or}$$

$$\tau_{xy} = K_1 \frac{S}{ba}.$$

The values of those non-dimensional coefficient  $K$  and  $K_1$  have been evaluated for different  $x/a$  between .5 and -.5. The shear stress ( $\tau_{xy}$ ) transverse stress ( $\sigma_y$ ), the shear (S) and moment (M) are calculated and then appropriate factors used to determine the stress at a particular point.

### Guyon's Theory

Another theoretical approach to the problem of calculating the stresses in an end block is due to Guyon (10, 11), who has obtained the analytical solution by the application of the infinite series. By the series solution, he could not satisfy all boundary conditions and therefore made some assumptions.

As a result of his complicated analysis, Guyon has given six tables for the calculation of  $\sigma_y$ ,  $\sigma_x$  and  $\tau_{xy}$  caused by normal or shear force in the anchorage zone. These tables make it possible to estimate the above mentioned stresses on nine vertical planes

$$y = -a, -\frac{3}{4}a, -\frac{1}{2}a, -\frac{1}{4}a, 0, \frac{1}{4}a, \frac{1}{2}a, \frac{3}{4}a, a,$$

at depths

$$x = 0, \frac{1}{6}a, \frac{1}{3}a, \frac{1}{2}a, \frac{2}{3}a, a, 1\frac{1}{2}a, 2a$$

for load at

$$y = 0, \frac{1}{4}a, \frac{1}{2}a, \frac{3}{4}a, a$$

The diagrams of the stress  $\sigma_y$  for various  $a_1/a$  ratios are shown in fig. 9.

Where  $a_1$  is half the width of the anchorage plate and  $a$  is half the width of the corresponding concrete prism.

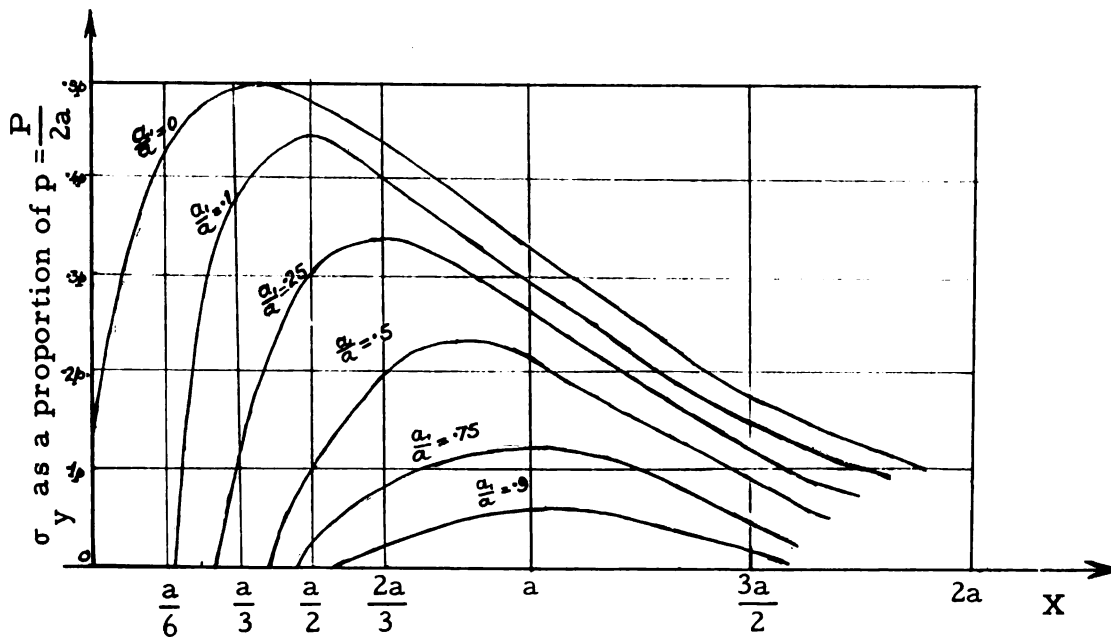


Fig. 9. Stress distribution according to Guyon's theory

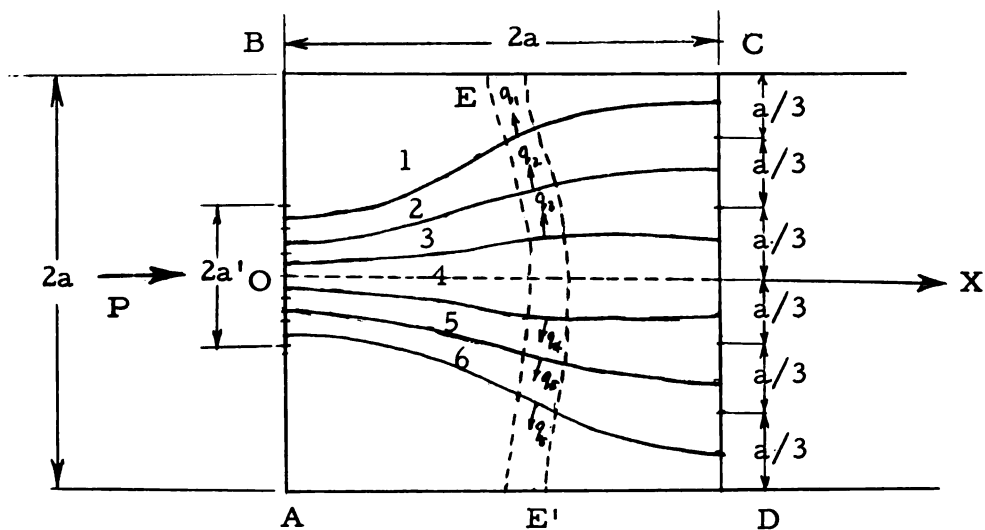


Fig. 10. Stress trajectories in Guyon's theory

Guyon carried out some tests on this subject, but he limited himself to a statement that the results given by this method agree very well with the photoelastic tests of Tessar (11).

In the text "Prestressed Concrete" published in 1953, Guyon has also given another approximate method of estimating the end block zone stresses using the isostatic lines approach. Here is an example of this method:

Case of a single axial force:--The single force  $P$  is uniformly distributed over a height  $2a'$  symmetrical about the axis of the beam  $OX$  (fig. 10). The forces can be considered as passing across the block from  $AB$  to  $CD$  along trajectories such as 1, 2, 3, 4, 5, and 6 in fig. 10. These trajectories are the isostatics issuing from the loaded area  $ab$ . These isostatics at their origin in  $ab$  are parallel to the force  $P$ , on their arrival at  $CD$  they are again parallel to  $P$ . Between these two sections, then, they must adopt an S-form with a point of inflection at  $I$ . Having divided  $ab$  and  $CD$  into  $n$  equal parts, each isostatic can be supposed to carry a force of  $\frac{P}{n}$  from the center of one division in  $ab$  to the center of the corresponding division in  $CD$ . The material in the interior of the zone may thus be considered as made up of a series of curved fibers, each carrying a fraction of the compressive force. Now these fibers cannot support compression without exerting a transverse force normal to each fiber caused by its curvature. This force acts inwards or outwards according to the direction of convexity of the curve. The traces of these transverse

forces are curves such as  $EE'$  normal to the thrust isostatics and form a second family of isostatics. They may be considered as dividing the material into another series of curved fibers tying together the first series and subjected to tension or compression by their transverse thrusts. Thus the tension of the fibers bounded by two curves  $EE'$  in fig. 10, increases from BC to OX, the thrusts  $q_1, q_2, q_3$  etc. due to each isostatic of the first family adding together as the band  $EE'$  crosses them successively and decreasing again between OX and AD in a similar manner. The transverse stresses are a maximum on the axis OX,  $\tau_{xy}$  by symmetry is zero on this axis. On the axis OX, therefore, the only stress is  $\sigma_y$  normal to the axis, its value varies from AB to CD at which point it becomes zero or at least negligible.

An idea of the variation of  $\sigma_y$  along OX may be gained by replacing the isostatics on each side of OX by an "average" isostatic carrying  $\frac{P}{2}$  to the center of the upper or lower half of CD (fig. 11). Then if R is the radius of curvature at any point M, the transverse force per unit of length of OX is  $\frac{P}{2R}$  and this transverse force per unit of length equals the stress  $\sigma_y$  since  $2b$  has been assumed to be unity. R is negative in the neighborhood of AB and  $\sigma_y$  is thus compressive. At I, R becomes infinite and  $\sigma_y$  is zero. Between I and CD, R becomes positive and  $\sigma_y$  becomes tensile, increasing until it reaches a maximum and then varying to zero as CD gets nearer.

The position of the point of zero stresses I, the value of maximum compressive stress near AB, and the value and position of the maximum

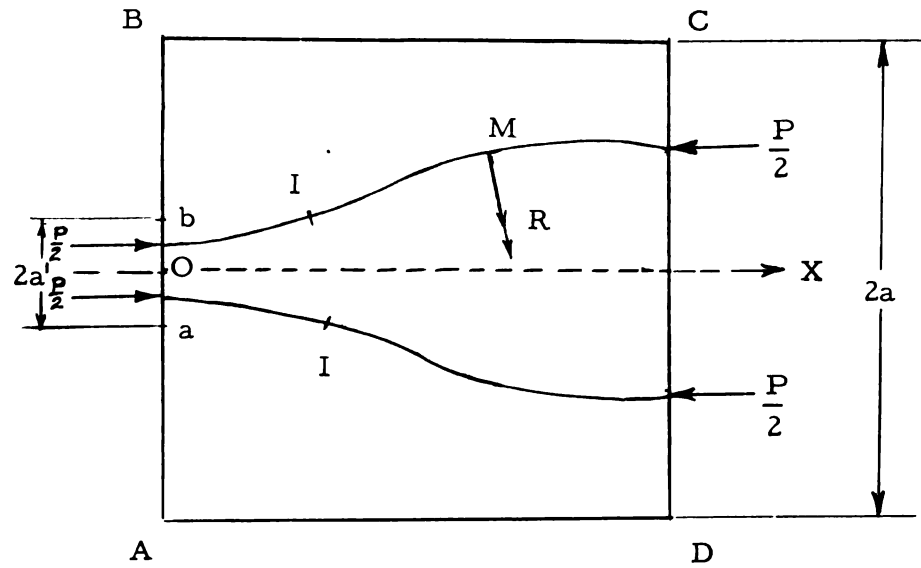


Fig. 11. Stress trajectories in Guyon's theory

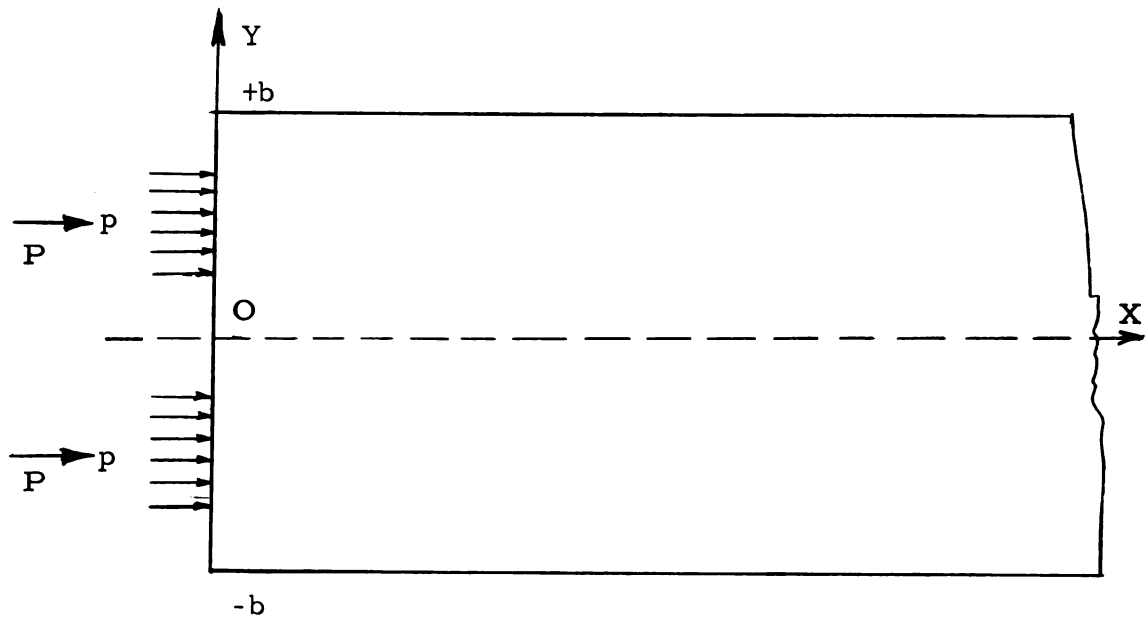


Fig. 12. Corresponding to Sundara Raja Iyenger's solution

tensile stress all depend on the ratio of the breadth  $2a'$  of the loaded band to the depth  $2a$  of the section

### Other Investigations

#### R. H. Carter's Study

The investigation of the same problem was carried out by R. H. Carter (5) at the University of Florida in 1952. The variation of stress in the end block was determined by actual test using Huggenberger tensometer for the strain measurements. The experimental results were compared with theoretical methods proposed by Prof. Gustav Magnel and by Boussinesq formula. Considerable variation between the three methods was reported. Of the three methods the results obtained by the Boussinesq formula were the least plausible, giving further evidence that the Boussinesq formula is not valid for finite areas. In the same paper Carter reported that the Magnel's assumption of the  $\sigma_x$  and  $\sigma_y$  stress distribution varied considerably from the experimental results. The experimental results were not absolutely reliable, however, it was evident the  $\sigma_x$  stress dispersed at an angle greater than 45 degrees and  $\sigma_y$  stresses did not always vary as a third degree parabola.

K. T. Sundara Raja Iyenger (12) solved the problem of stress distribution in the anchorage zone by series method. He used the Airy Stress function approach to deal with the problem as a two dimensional (fig. 12) elasticity problem. He starts by assuming a stress function

$$\phi = -\frac{P}{2b} y^2 + \sum_{n=1,2,3}^{\infty} \frac{B_n \cos \frac{n\pi y}{b}}{\left(\frac{n\pi}{b}\right)^2} \left[1 + \frac{n\pi x}{b}\right] e^{-\frac{n\pi x}{b}} \quad (1)$$

$$+ \int_0^{\infty} \frac{A(a) \cos ax}{a^2 \cosh ab} [ay \sinh ay - (1+ab \coth ab) \cosh ay] da$$

to satisfy the differential equation

$$\frac{\partial^4 \phi}{\partial x^4} + 2 \frac{\partial^4 \phi}{\partial x^2 \partial y^2} + \frac{\partial^4 \phi}{\partial y^4} = 0 \quad (2)$$

The solution of the problem is then subject to the boundary conditions

$$\begin{aligned} \sigma_y &= 0 \text{ at } y = \pm b \\ \tau_{xy} &= 0 \text{ at } y = \pm b \text{ and } x = 0 \\ \left. \begin{aligned} \sigma_x &= -p(y) \text{ at } x = 0 \\ &= -\frac{P}{b} \text{ at } x \rightarrow \infty \end{aligned} \right\} \text{Where } p(y) \text{ is given.} \end{aligned} \quad (3)$$

Applying the above boundary conditions the set of coefficients in equation (1) have been evaluated by using Crouts method. However the same could be done quite easily by using digital computer.

### Bleich's and Siever's Theories

The next theories on stress analysis under concentrated loads are those given by Bleich (2) and Sievers (20, 21). Although these theories

were not derived primarily for calculation of the stresses in the anchorage zone, both theories deserve careful examination. Sievers followed in principle the Mörsch's approach to the problem, making use of an analysis by Bleich of deep beams.

In this analysis Bleich makes use of an Airy Stress function  $F$  such that

$$\sigma_y = \frac{\partial^2 F}{\partial x^2} ; \sigma_x = \frac{\partial^2 F}{\partial y^2} ; \tau_{xy} = \frac{\partial^2 F}{\partial x \partial y}$$

Satisfying the governing equation

$$\frac{\partial^4 F}{\partial x^4} + \frac{2\partial^4 F}{\partial x^2 \partial y^2} + \frac{\partial^4 F}{\partial y^4} = 0$$

for the case of symmetrical load shown in fig. 13, the stresses are given

by:

$$\sigma_y = 2 \frac{P}{a} \sum_{n=1}^{\infty} \frac{(1 - \beta_n h) \cosh \beta_n x + \beta_n x \sinh \beta_n x}{e^{\beta_n h}} \cos \beta_n y$$

where

$$\beta_n = \frac{n\pi}{a}$$

To satisfy the boundary conditions, it was shown by Bleich that the modified equation

$$\sigma_y = 2 \sum_{n=1, 3, 5}^{\infty} \frac{P}{2at} [1 - \beta_n (h - x)] e^{-\beta_n (h - x)}$$

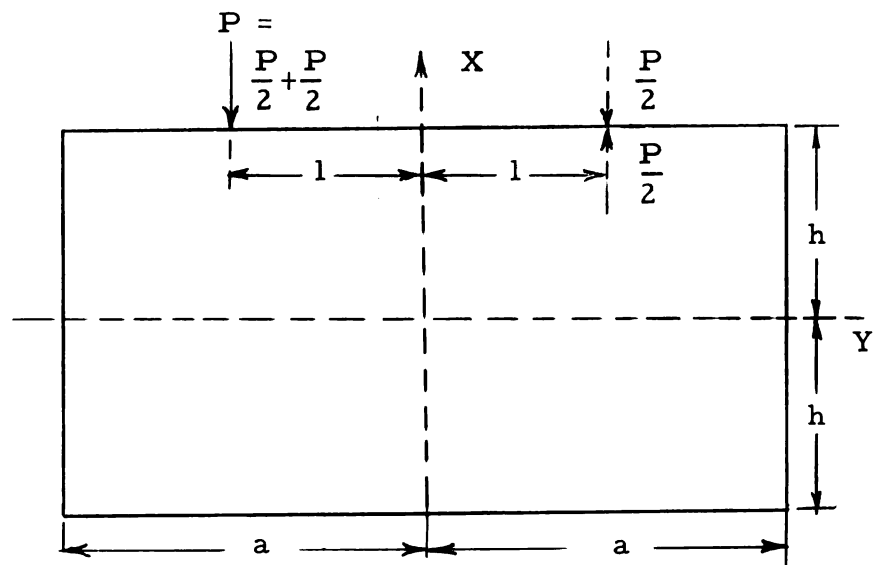


Fig. 13. Symmetrical load in Bleich's theory

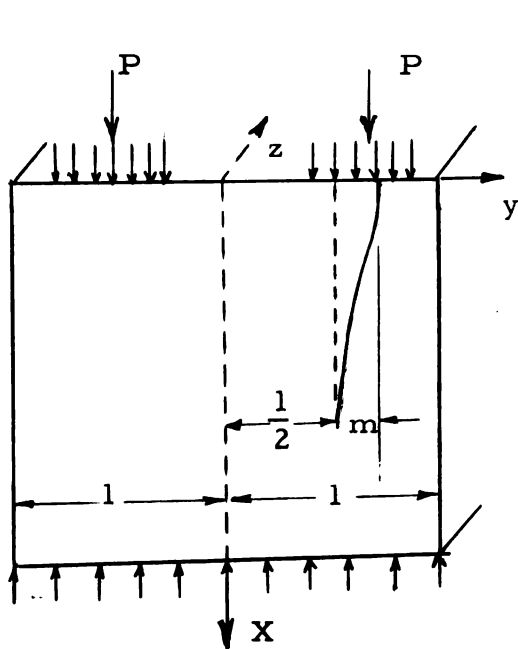


Fig. 14a. Notation for Siever's formula

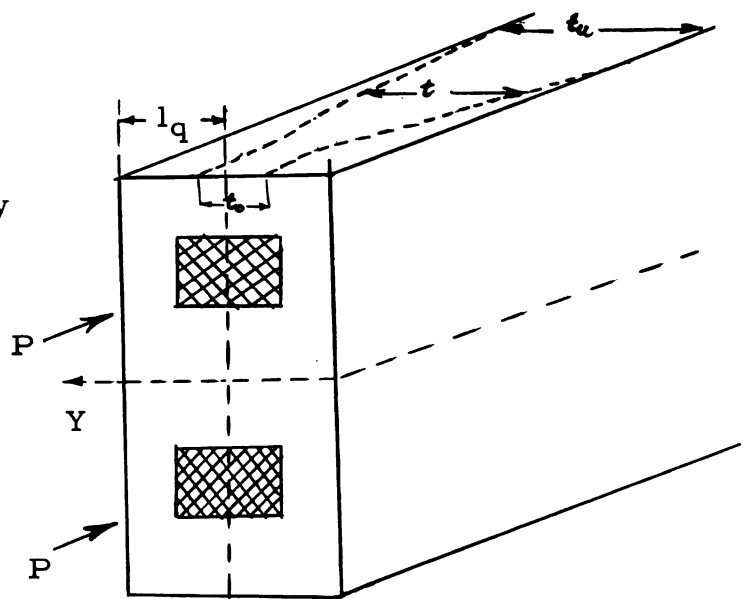


Fig. 14b. Variation of  $t$  in the end block

should be used for plane  $y = 0$ . Sievers also presented an approximate formula for the evaluation of the transverse stresses which fulfilled the required boundary condition. With the notation given in fig. 14a

$$\sigma_y = \frac{8Pm}{tl^2} (1 - 2.5\eta) e^{-(\pi/2)1.6\eta_q}$$

where

$$\eta = x/l \text{ and}$$

$t$  = the variable width at which the load acts in the direction  $Z$ . The variation of  $t$  as a function of the length of the end block is expressed by the equation

$$t = t_o - 2m_q (1 + 2.5\eta_q) e^{-(\pi/2)1.6\eta_q}$$

where

$$m_q = .5(t_u - t_o)$$

and

$$\eta_q = x/l_q$$

fig. 14b represents the variation of  $t$  in the end block.

Photoelastic tests carried out by Hirschfeld (21) at Aachen in connection with the design of bridge piers confirm the qualitative results of the Bleich-Sievers theory. The total tensile force calculated according to Sievers stress distribution is about 17 % higher than that given by Mörsch's theory.

### Existing Test Data on Stresses in Anchorage Zone

More recent tests have been carried out on the problem of stress distribution in post-tensioned members by Christodoulides (6), (1955) and Ban (1), (1957).

Christodoulides's preliminary tests on stress distribution in anchorage zones were carried out as two-dimensional problems in which standard photoelastic techniques were employed.

For the three dimensional photo-elastic investigation as applied to a model of an actual end block, he used the frozen stress technique. The analysis of the experimental data enabled Christodoulides to point out for the first time that the existing methods of estimating tensile stresses in the end block underestimated the actual values and hence, special attention should be paid to this problem.

Christodoulides (7) drew the following conclusions on the basis of photoelastic tests as well as on stress analysis in the full scale concrete gantry beam, where strain in three directions was measured by means of embedded strain gages.

(1) The maximum principal tensile stress occurs near the loaded end face on the central axis of the prism, between the anchorages.

(2) The values of the stresses expressed in terms of uniform compression based on the three-dimensional stress :

maximum shear stress = 2 x uniform compression

maximum principal compression = 4 x uniform compression

maximum principal tensile stress = .6 x uniform compression.

The three dimensional stress distribution obtained by photoelastic methods on models agreed satisfactorily with the results calculated from strain measurements. but not with the Magnels and Guyon's theories . This indicates that the effect of Poisson's ratio on the stresses is small.

Christodoulides in his tests neglected such factors as cable ducts and embedded anchorages because of technical difficulties. These may have had a quantitative influence on the distribution of tensile stresses in the end anchorages.

Ban (1) and his team recognized the importance of the individual method of post-tensioning for the values and distribution of tensile stresses in the anchorage zone. They worked with a particular method of post-tensioning, namely the Lee-McCall method. Apart from analyzing the position and magnitude of stresses and comparing these with the theoretical values they investigated the influence of specific factors upon the stress distribution as well as upon cracking and ultimate load. Some of these specific factors were:

- (1) ratio of the dimensions of the anchorage plate to those of corresponding concrete;
- (2) the thickness of the anchorage plate;
- (3) the dimensions of the anchorage nut ;
- (4) the amount and position of reinforcement ;
- (5) the strength of the concrete;

Strains were measured by means of electric strain gages on 40 rectangular concrete end blocks 20.8" in depth and  $7\frac{1}{8} \times 4\frac{3}{4}$  inches in cross section.

Ban pointed out the following

(1) Measured strain distribution decreased markedly from that given by Guyon and Magnel .

(2) Measured strains agreed fairly well with the Bleich-Sievers theory.

(3) Poissons ratio influenced the agreement measured and theoretical strains.

(4) Cracking load of the anchorage end block of Lee-McCall post-tensioned beams remained approximately constant regardless of the surface area of the anchorage plate. It might be influenced by the thickness of plate and the nut.

(5) Amount of transverse reinforcement had a considerable effect on the cracking load.

(6) The linear relationship between the strength of concrete, or the thickness of the anchorage plate, and the cracking and ultimate load was recognized.

#### Cement and Concrete Association Research (23)

In September 1960, the Cement and Concrete Association, London, England, published a research report reviewing the existing theoretical and experimental work. The report shows that wide differences exist among the

various theories. The measurements performed by the C. C. A. were executed in two stages. The first series of tests dealt with the problem of individual end blocks subjected to single, symmetrically placed concentrated loads and the second series dealt with the interaction effects when numbers of concentrated forces acted on a single end block of varying cross sections.

The variables studied included the ratio of the loaded area to the cross sectional area, the type of anchorage (whether embedded or external), the effect of ducts, and the percentage and form of reinforcement. The results obtained are compared with those predicted by the existing theories; the theories due to Guyon and Magnel underestimate the maximum experimental tensile stresses by a percentage varying between 160 and 280 for various ratios of loaded area to cross-sectional area. An empirical method, based upon the experimental results obtained, is suggested for determining the total tensile force and its distribution in an end block.

Their recommendations are based on the same approach as was suggested by Guyon, but whereas he applied it to theoretical values, it is applied here to the experimental results, showing the distribution of the transverse stresses in the anchorage zone.

The important conclusions which have been drawn as a result of the above research need mention here.

(1) The distribution of transverse stress and the ultimate load of an end block are not altered significantly by the different types and shapes of anchorages.

(2) An important factor in the distribution of transverse stress and the ultimate load is the ratio of the loaded area to the cross-sectional area of the prism.

(3) The positions of maximum and zero transverse stresses are not significantly affected by  $a_1/a$  ratio.

(4) The maximum transverse stresses, which always occur on the central axis of the prism, are greater than those predicted by any other existing theories.

These stresses are expressed as a fraction of the uniform compressive stresses

$$.73 \text{ for } a_1/a = .30$$

$$.40 \text{ for } a_1/a = .70$$

(5) Theories due to Bleich and Sievers give the closest approximation. Other theories do not give satisfactory assessment of the stresses.

(6) The total value of transverse tensile force, which is independent of the width of the end block is given by

$$.36 P \text{ for } a_1/a = .30$$

$$.20 P \text{ for } a_1/a = .70$$

TABLE 1. Comparison of theoretical results<sup>1</sup>

	Theory due to					
	Mörsch	Bortsch	Magnel	Magnel modified	Guyon	Bleich Sievers
$a_1 / a$	0-1.0	0-0.20	0-1.0	0-1.0	0.10-0.90	0.10-0.90 0.30-0.70
Distance of maximum tensile stresses from the loaded face in terms of a	1.00	0.40-0.60	1.00	1.33	0.50-0.90	0.50-0.60 0.50-0.60
Distance of zero tensile stresses in terms of a	0	0.20-0.25	0.50	0.66	0.45-0.20	0.20-0.32 0.30
Distance of uniform compressive stresses in terms of a	2.0	3.4	2.0	2.0	2.0	2.0 2.0
Value of maximum tensile stress as a ratio of uniform compression	(for $a_1/a$ -0.30-0.70) 0.26-0.16	0.45-0.38	(for $a_1/a$ -0.30-0.70) 0.43-0.22	(for $a_1/a$ -0.30-0.70) 0.30-0.70	0.42-0.04	0.59-0.07 0.71-0.26
$2a$ = width of prism						

<sup>1</sup>J. Zielinski and R. E. Rowe, Cement and Concrete Association, Research Report 9, September, 1960, p. 7.

(7) At the cracking load the uniform compression expressed as a fraction of the corrected compressive strength was .16 and .28 for  $a_1/a$  ratios of .30 and .70 respectively.

(8) The percentage of reinforcement has a significant effect on the bearing capacity of end blocks for values of the contact stresses up to 1.9 times the cube strength. There is no increase in the bearing capacity if the reinforcement is increased, when the contact stresses are in the range of 1.9 to 3.4 times the cube strength.

(9) The reinforcement is required primarily in the region of the end block extending from .2a to 1.0a. The tests showed that helical reinforcement was more efficient than mat reinforcement.

A comparison between various theories has been made as given in Table 1, page 30.

### III SCOPE OF INVESTIGATION

From the review of the literature, it seems that an exact analytical solution has not been developed which will satisfy all of the boundary conditions. While various types of series solutions have been obtained, the accuracy of these results depends upon the number of terms taken. Moreover these series solutions may not satisfy all of the boundary conditions.

In elasticity problems the finite difference approach is being used more and more. This approach satisfies all boundary conditions. The accuracy depends upon the fineness of the finite difference grid. The finer the grid, the greater is the number of the linear simultaneous algebraic equations to be solved. The solution of these equations is no more a problem and can be easily solved by using the high speed digital computer.

If the bearing plate extends across the width of the member the beam may be considered to have a line load and be analyzed as a two-dimensional stress problem. No attempt is made in this paper to treat the problem as a three-dimensional one.

The analysis was carried out with the following assumptions:

- (1) Ducts of cables are neglected
- (2) State of plane stress exists
- (3) All elasticity laws are valid (though it may not be very justified as concrete has aggregate which might affect the distribution of stress.)

(4) Prestressing force is distributed uniformly through the bearing plate (which depends upon the thickness of plate used).

The first and second assumptions are justified only if the ducts areas are small compared to the cross section and the width of the section is small.

To summarize, this investigation is intended to investigate the following:

(1) What is the distribution of stress at the ends of post-tensioned member?

(2) Are built up sections needed in post-tensioned members?

## IV THEORETICAL INVESTIGATION

The solution of a two-dimensional problem involves the integration of the differential equations of equilibrium together with the compatibility equation and the boundary conditions. If we begin with the case where the weight of the body is the only body force, the equations to be satisfied are as follows:

$$\frac{\partial \sigma_x}{\partial x} + \frac{\partial \tau_{xy}}{\partial y} = 0 \quad \text{--- (a)}$$

$$\frac{\partial \sigma_y}{\partial y} + \frac{\partial \tau_{xy}}{\partial x} + g = 0$$

$$\left[ \frac{\partial^2}{\partial x^2} + \frac{\partial^2}{\partial y^2} \right] (\sigma_x + \sigma_y) = 0 \quad \text{--- (b)}$$

to these equations, boundary condition equations (c) are added:

$$\begin{aligned} \bar{x} &= l\sigma_x + m\tau_{xy} \\ \bar{y} &= m\sigma_y + l\tau_{xy} \end{aligned} \quad \text{--- (c)}$$

where  $\bar{x}$  and  $\bar{y}$  are the components of the surface force per unit area,  $l$  and  $m$  are the direction cosines of the normal to the boundary.

A function called Airy's stress function is introduced at this stage to solve these equations. Then the stresses are given by the partial derivatives of this stress function.

$$\sigma_x = \frac{\partial^2 \phi}{\partial y^2} - \rho gy$$

$$\sigma_y = \frac{\partial^2 \phi}{\partial x^2} - \rho g y$$

and

--- (d)

$$\tau_{xy} = -\frac{\partial^2 \phi}{\partial x \partial y}$$

defining the stresses in this manner the equilibrium equations (a) are identically satisfied. The solution of the problem is that which satisfies also the compatibility condition (b). Therefore the stress function ( $\phi$ ) must satisfy the equation

$$\frac{\partial^4 \phi}{\partial x^4} + 2 \frac{\partial^4 \phi}{\partial x^2 \partial y^2} + \frac{\partial^4 \phi}{\partial y^4} = 0 \quad \text{--- (e)}$$

when the weight is the only body force, the solution of the two-dimensional problem reduces to finding a solution to equation (e) which satisfies the boundary conditions of the problem.

The finite difference method affords a good technique of solving these equations with the help of a high speed digital computer. Here the differential equation is replaced by the corresponding finite difference equation at each point of the grid.

The finite difference pattern for the biharmonic equation is shown in fig. 15

$$\frac{\partial^4 \phi}{\partial x^4} + 2 \frac{\partial^4 \phi}{\partial x^2 \partial y^2} + \frac{\partial^4 \phi}{\partial y^4} = 0.$$

This finite difference equation must be satisfied at every nodal point of the

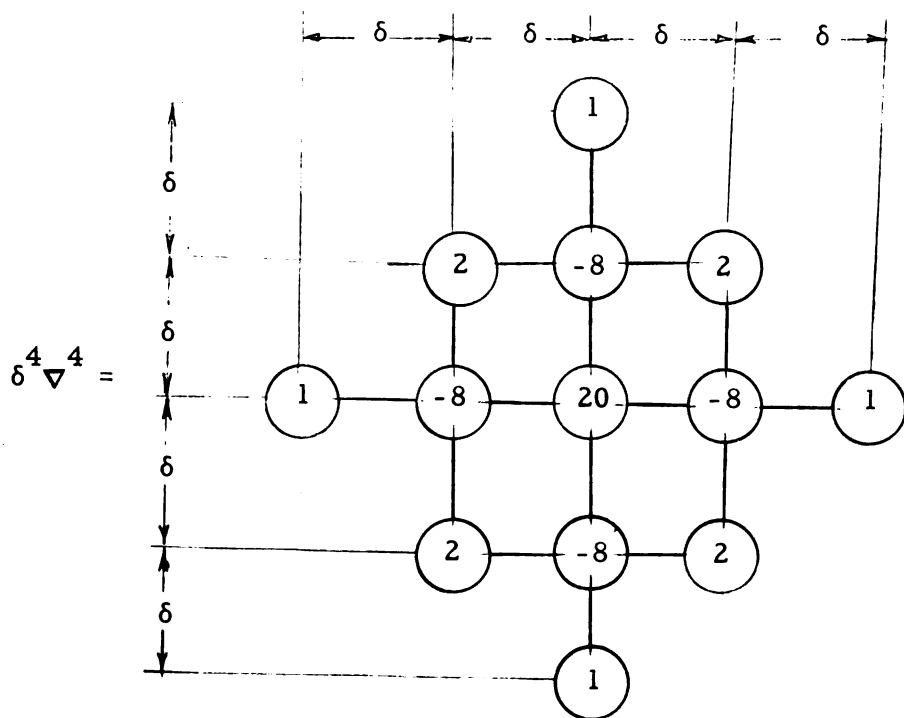


Fig. 15 Finite difference pattern for the biharmonic equation

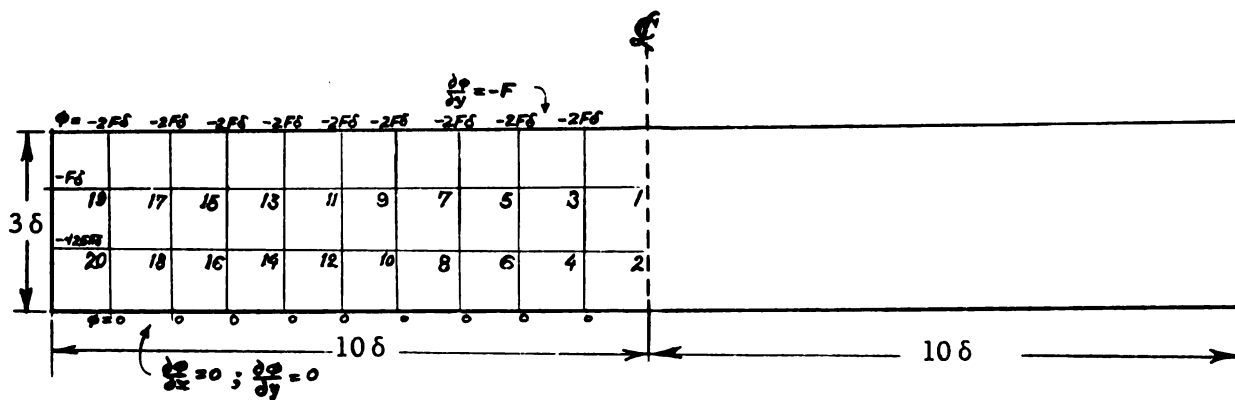


Fig 16. Finite difference grid and boundary values

grid within the boundary of the plate. The boundary values of the stress function  $\phi$  have to be determined using the given boundary conditions.

A beam of depth to length ratio 3:20 is shown in fig. 16. Since it is known from the principle of St. Venant that stress distribution is linear at some distance from the concentrated force, this ratio should be sufficient to cover the stress concentration effect.

### $\phi$ Values at the Boundary

Along the bottom surface there is no force, hence (fig. 16):

$$\frac{\partial^2 \phi}{\partial x^2} = \sigma_y = 0 \text{ (normal stress)}$$

$$-\frac{\partial^2 \phi}{\partial x \partial y} = \tau_{xy} = 0 \text{ (shear stress)}$$

It is assumed that the prestressing force is distributed over  $.1L = \delta$  through the bearing plates.

From the above we obtain

$$\phi = 0, \quad \frac{\partial \phi}{\partial y} = 0$$

choosing the arbitrary constants in such a way to make them true.

Along the ends up to  $\frac{\delta}{2}$ , there is no stress, therefore  $\phi = 0, \frac{\partial \phi}{\partial y} = 0$  (no change).

For the portion under the bearing plate we have

$$\frac{\partial^2 \phi}{\partial y^2} = -\frac{F}{.1L} = -\frac{10F}{L} \text{ and } -\frac{\partial^2 \phi}{\partial x \partial y} = 0$$

because there is no shearing stress there.

Integrating once we have

$$\frac{\partial \phi}{\partial y} = \frac{-10F}{L} y + A = -\frac{F}{\delta} y + A$$

changing .1L to  $\delta$  and integrating once again

$$\phi = -\frac{Fy^2}{2\delta} + Ay + B$$

and  $\frac{\partial \phi}{\partial x} = \text{constant} = 0$ , as before.

Since we have for vertical side up to  $y = \delta/2$

$$\frac{\partial^2 \phi}{\partial y^2} = 0, \quad \frac{\partial \phi}{\partial y} = \text{constant}$$

$$-\frac{\partial^2 \phi}{\partial x \partial y} = 0, \quad \frac{\partial \phi}{\partial x} = \text{constant}$$

In this case both the constants are equal to zero.

$$\phi \text{ for } \frac{\delta}{2} < y < \frac{3\delta}{2}$$

Now to evaluate the constants A and B we proceed as follows:

Since at  $y = .5\delta$  we have  $\phi = 0$ ,  $\frac{\partial \phi}{\partial y} = 0$ , therefore

$$A = \frac{F}{\delta} y = \frac{F}{\delta} (.5\delta) = 0.5F$$

then

$$\phi = -\frac{F}{\delta} \frac{y^2}{2} + .5 Fy + B$$

or

$$\begin{aligned} B &= \frac{F}{\delta} \frac{.25}{2} \delta^2 - .5F (.5\delta) \\ &= .125 F\delta - .25 F\delta = -.125 F\delta \end{aligned}$$

Therefore the expression for  $\phi$  becomes

$$\phi = \frac{-F}{2\delta} y^2 + .5 Fy - .125 F\delta$$

for

$$.5\delta < y < 1.5\delta$$

then

$$\begin{aligned} \left. \phi \right]_{1.5\delta} &= \frac{-F}{2\delta} (1.5\delta)^2 + .5F(1.5\delta) - .125 F\delta \\ &= -1.125 F\delta + .75 F\delta - .125 F\delta \\ &= -.5 F\delta \text{ at } y = 1.5\delta \end{aligned}$$

also

$$\begin{aligned} \left. \phi \right]_{\delta} &= \frac{-F}{2\delta} \delta^2 + .5F\delta - .125 F\delta \\ &= -.125 F\delta \text{ at } y = \delta \end{aligned}$$

for the portion  $y > 1.5\delta$ , there is no load again, hence

$$\frac{\partial^2 \phi}{\partial y^2} = 0, \quad \frac{\partial^2 \phi}{\partial x \partial y} = 0$$

From the previous portion we already have

$$\frac{\partial \phi}{\partial y} = \frac{-F}{\delta} y + .5F$$

$$\left. \frac{\partial \phi}{\partial y} \right]_{1.5\delta} = \frac{-F}{\delta} y + .5F$$

$$= -1.5F + .5F = -F$$

Then integrating the expressions

$$\frac{\partial \phi}{\partial y} = C \text{ but } C = -F \text{ as at } y = 1.5\delta, \frac{\partial \phi}{\partial y} = -F \text{ (as found before)}$$

Integrating further

$$\phi = Cy + D$$

$$\phi = -Fy + D$$

but

$$\phi = -.5F\delta \text{ at } y = 1.5\delta$$

then

$$-.5F\delta = -F(1.5\delta) + D$$

so

$$D = F\delta$$

and

$$\phi = -Fy + F\delta$$

for  $1.5 < y < 3\delta$

$$\begin{aligned} \text{therefore } \left. \phi \right]_{3\delta} &= -3F\delta + F\delta \\ &= -2F\delta \text{ at } y = 3\delta \end{aligned}$$

and

$$\begin{aligned} \left. \phi \right]_{2\delta} &= -2F\delta + F\delta \\ &= -F\delta \text{ at } y = 2\delta \end{aligned}$$

Now for the top surface, again there is no load

$$\text{therefore } \frac{\partial^2 \phi}{\partial x^2} = 0, -\frac{\partial^2 \phi}{\partial x \partial y} = 0$$

Integrating we obtain

$$\frac{\partial \phi}{\partial x} = 0, \text{ (constant, as found before)}$$

$$\frac{\partial \phi}{\partial y} = -F \text{ (constant, as found before)}$$

at the corner the value of  $\frac{\partial \phi}{\partial y}$  must be the same for both sides.

Therefore we have the condition summed up as follows at the corner :

$$\left. \begin{array}{l} \phi = \text{constant} = -2F\delta \\ \frac{\partial \phi}{\partial y} = \text{constant} = -F \end{array} \right\} \text{ at } y = 3\delta$$

Since because of symmetry we do not need to go through the right hand portion of the boundary but still it will be evaluated to serve as a check.

### Right Hand Vertical Face

We have

$$\frac{\partial^2 \phi}{\partial y^2} = 0, \frac{\partial^2 \phi}{\partial x \partial y} = 0$$

then

$$\begin{aligned} \frac{\partial \phi}{\partial y} &= \text{constant} \\ &= -F \end{aligned}$$

and

$$\frac{\partial \phi}{\partial x} = \text{constant} = 0$$

also

$$\phi = -Fy + \text{constant}$$

Since for the top corner at  $y = 3\delta$  we have  $\phi = -2\delta F$ , therefore

$$\left. \begin{aligned} \phi &= -2\delta F = -3\delta F + \text{constant} \\ \text{constant} &= F\delta \end{aligned} \right\} \text{at } y = 3\delta$$

then

$$\phi = -Fy + F\delta$$

now at

$$y = 1.5\delta$$

$$\phi = -F(1.5\delta) + F\delta$$

$$\left. \begin{aligned} \phi &= -.5 F\delta \\ \frac{\partial \phi}{\partial y} &= -F \end{aligned} \right\} \text{at } y = 1.5\delta$$

Then for  $y = 1.5\delta$  to  $.5\delta$  we have

$$\frac{\partial^2 \phi}{\partial y^2} = \frac{-F}{\delta}$$

$$-\frac{\partial^2 \phi}{\partial x \partial y} = 0; \quad \frac{\partial \phi}{\partial x} = \text{constant} = 0$$

therefore

$$\frac{\partial \phi}{\partial y} = -\frac{F}{\delta} y + \text{constant}$$

now at

$$y = 1.5\delta$$

$$\frac{\partial\phi}{\partial y} = -F$$

then

$$-F = -\frac{F}{\delta} (1.5\delta) + \text{constant (E)}$$

therefore

$$E = .5F$$

and we have

$$\frac{\partial\phi}{\partial y} = \frac{-F}{\delta} y + .5F$$

$$\phi = \frac{-F}{2\delta} y^2 + .5Fy + \text{constant (G)}$$

now at

$$y = 1.5\delta$$

$$\phi = -.5F\delta$$

$$-.5F\delta = \frac{-F}{2\delta} (2.25\delta^2) + .5F(1.5\delta) + G$$

$$-.5\delta F = -1.125F\delta + .75F\delta + G$$

or

$$G = -.125F\delta$$

then

$$\phi = \frac{-F}{2\delta} y^2 + .5Fy - .125F\delta$$

check:

$$\text{at } y = .5\delta$$

$$\begin{aligned}\phi &= \frac{-F}{2\delta} (.25) \delta^2 + .5 F(.5\delta) - .125 F\delta \\ &= -.125F\delta + .25 F\delta - .125 F\delta = 0\end{aligned}$$

similarly

$$\frac{\partial \phi}{\partial y} = -\frac{F}{\delta} (.5\delta) + .5 F = 0$$

therefore

$$\left. \begin{aligned}\phi &= 0 \\ \frac{\partial \phi}{\partial y} &= 0 \\ \frac{\partial \phi}{\partial x} &= 0\end{aligned} \right\} \text{ at } y = .5\delta \text{ and below}$$

Again for the lower portion we have

$$\frac{\partial^2 \phi}{\partial y^2} = 0 ; -\frac{\partial^2 \phi}{\partial x \partial y} = 0$$

since there is no load.

And we obtain

$$\frac{\partial \phi}{\partial y} = \text{const.} = 0$$

$$\phi = \text{const.} = 0$$

for the bottom side again since there is no load we have

$$\frac{\partial^2 \phi}{\partial x^2} = 0 ; -\frac{\partial^2 \phi}{\partial x \partial y} = 0$$

$$\frac{\partial \phi}{\partial x} = 0 ; \frac{\partial \phi}{\partial y} = \text{const.}$$

as at the lower corner.

The value of  $\phi$ ,  $\frac{\partial \phi}{\partial y}$  and  $\frac{\partial \phi}{\partial x}$  are noted below along the boundaries (fig. 16).

The  $\phi$  (stress function) values along the boundary of the beam are thus known and they have been indicated along the boundary in the fig. 16.

Now the finite difference equation for each point of the grid in turn are written as follows:

for point 1  $21\phi_1 - 8\phi_2 - 16\phi_3 + 4\phi_4 + 2\phi_5 = -6F\delta$

for point 2

$$-8\phi_1 + 21\phi_2 + 4\phi_3 - 16\phi_4 + 2\phi_6 = 2F\delta$$

for point 3

$$-8\phi_1 + 2\phi_2 + 22\phi_3 - 8\phi_4 - 8\phi_5 + 2\phi_6 + \phi_7 = -6F\delta$$

for point 4

$$2\phi - 8\phi_2 - 8\phi_3 + 22\phi_4 + 2\phi_5 - 8\phi_6 + \phi_8 = 2F\delta$$

for point 5

$$\phi_1 - 8\phi_3 + 2\phi_4 + 21\phi_5 - 8\phi_6 - 8\phi_7 + 2\phi_8 + \phi_9 = -6F\delta$$

for point 6

$$\phi_2 + 2\phi_3 - 8\phi_4 - 8\phi_5 + 21\phi_6 + 2\phi_7 - 8\phi_8 + \phi_{10} = 2F\delta$$

for point 7

$$\phi_3 - 8\phi_5 + 2\phi_6 + 21\phi_7 - 8\phi_8 - 8\phi_9 + 2\phi_{10} + \phi_{11} = -6F\delta$$

for point 8

$$\phi_4 + 2\phi_5 - 8\phi_7 + 21\phi_8 + 2\phi_9 - 8\phi_{10} + \phi_{12} = 2F\delta$$

for point 9

$$\phi_5 - 8\phi_7 + 2\phi_8 + 21\phi_9 - 8\phi_{10} - 8\phi_{11} + 2\phi_{12} + \phi_{13} = -6F\delta$$

for point 10

$$\phi_6 + 2\phi_7 - 8\phi_8 - 8\phi_9 + 21\phi_{10} + 2\phi_{11} - 8\phi_{12} + \phi_{14} = 2F\delta$$

for point 11

$$\phi_7 - 8\phi_9 + 21\phi_{11} - 8\phi_{12} - 8\phi_{13} + 2\phi_{14} + \phi_{15} = -6F\delta$$

for point 12

$$\phi_8 + 2\phi_9 - 8\phi_{10} - 8\phi_{11} + 21\phi_{12} + 2\phi_{13} - 8\phi_{14} + \phi_{16} = 2F\delta$$

for point 13

$$\phi_9 - 8\phi_{11} + 2\phi_{12} + 21\phi_{13} - 8\phi_{14} - 8\phi_{15} + 2\phi_{16} + \phi_{17} = -6F\delta$$

for point 14

$$\phi_{10} + 2\phi_{11} - 8\phi_{12} - 8\phi_{13} + 21\phi_{14} + 2\phi_{15} - 8\phi_{16} + \phi_{18} = 2F\delta$$

for point 15

$$\phi_{11} - 8\phi_{13} + 2\phi_{14} + 21\phi_{15} - 8\phi_{16} - 8\phi_{17} + 2\phi_{18} + \phi_{19} = -6F\delta$$

for point 16

$$\phi_{12} + 2\phi_{13} - 8\phi_{14} - 8\phi_{15} + 21\phi_{16} + 2\phi_{17} - 8\phi_{18} + \phi_{20} = 2F\delta$$

for point 17

$$\phi_{13} - 8\phi_{15} + 2\phi_{16} + 21\phi_{17} - 8\phi_{18} - 8\phi_{19} + 2\phi_{20} = -5F\delta$$

for point 18

$$\phi_{14} + 2\phi_{15} - 8\phi_{16} - 8\phi_{17} + 21\phi_{18} + 2\phi_{19} - 8\phi_{20} = 2.125F\delta$$

Table 2

## Matrix

	$\phi$																				
No	1	2	3	4	5	6	7	8	9	10	11	12	13	14	15	16	17	18	19	20	F $\delta$
1	10.5	-4	-8	2	1	0	0	0	0	0	0	0	0	0	0	0	0	0	0	0	3
2	-4	10.5	2	-8	0	1	0	0	0	0	0	0	0	0	0	0	0	0	0	0	-1
3	-8	2	22	-8	-8	2	1	0	0	0	0	0	0	0	0	0	0	0	0	0	6
4	2	-8	-8	22	2	-8	0	1	0	0	0	0	0	0	0	0	0	0	0	0	-2
5	1	0	-8	2	21	-8	-8	2	1	0	0	0	0	0	0	0	0	0	0	0	6
6	0	1	2	-8	-8	21	2	-8	0	1	0	0	0	0	0	0	0	0	0	0	-2
7	0	0	1	0	-8	2	21	-8	-8	2	1	0	0	0	0	0	0	0	0	0	6
8	0	0	0	1	2	-8	-8	21	2	-8	0	1	0	0	0	0	0	0	0	0	-2
9	0	0	0	0	1	0	-8	2	21	-8	-8	2	1	0	0	0	0	0	0	0	6
10	0	0	0	0	0	1	2	-8	-8	21	2	-8	0	1	0	0	0	0	0	0	-2
11	0	0	0	0	0	0	1	0	-8	2	21	-8	-8	2	1	0	0	0	0	0	6
12	0	0	0	0	0	0	0	1	2	-8	-8	21	2	-8	0	1	0	0	0	0	-2
13	0	0	0	0	0	0	0	0	1	0	-8	2	21	-8	-8	2	1	0	0	0	6
14	0	0	0	0	0	0	0	0	0	1	2	-8	-8	21	2	-8	0	1	0	0	-2
15	0	0	0	0	0	0	0	0	0	0	1	0	-8	2	21	-8	-8	2	1	0	6
16	0	0	0	0	0	0	0	0	0	0	0	1	2	-8	-8	21	2	-8	0	1	-2
17	0	0	0	0	0	0	0	0	0	0	0	0	1	0	-8	2	21	-8	-8	2	5
18	0	0	0	0	0	0	0	0	0	0	0	0	0	1	2	-8	-8	21	2	-8	-2.125
19	0	0	0	0	0	0	0	0	0	0	0	0	0	0	1	0	-8	2	22	-8	13.75
20	0	0	0	0	0	0	0	0	0	0	0	0	0	0	0	1	2	-8	-8	22	-3

for point 19

$$\phi_{15} - 8\phi_{17} + 2\phi_{18} + 22\phi_{19} - 8\phi_{20} = -13.75F\delta$$

for point 20

$$\phi_{16} + 2\phi_{17} - 8\phi_{18} - 8\phi_{19} + 22\phi_{20} = 3F\delta$$

These simultaneous equations are written in the form of

$$\sum_{i, j, = 0}^{n-1} a_{ij} x + a_{in} = 0$$

and entered in a table in the matrix form, and this matrix should ordinarily be a symmetrical matrix, which serves as a check, that the finite difference equations have been formulated correctly. The first two equations no. 1 and 2, have to be divided throughout by 2 to make the matrix symmetrical.

Data was fed to the Mystic Computer and the solution of the equations for the values of  $\phi$  was given by the computer as given below:

$\phi_1$	=	-1.0303046
$\phi_2$	=	-0.3030319
$\phi_3$	=	-1.0303079
$\phi_4$	=	-0.3030351
$\phi_5$	=	-1.0303219
$\phi_6$	=	-0.3030486
$\phi_7$	=	-1.0303586
$\phi_8$	=	-0.3030820
$\phi_9$	=	-1.0304229
$\phi_{10}$	=	-0.3031252
$\phi_{11}$	=	-1.0304276

$\phi_{12}$	=	-0.3030130
$\phi_{13}$	=	-1.0298987
$\phi_{14}$	=	-0.3018938
$\phi_{15}$	=	-1.0273002
$\phi_{16}$	=	-0.2965732
$\phi_{17}$	=	-1.0195047
$\phi_{18}$	=	-0.2775298
$\phi_{19}$	=	-1.0052337
$\phi_{20}$	=	-0.2239330

Calculation of Stresses

$\sigma_x = \frac{\partial^2 \phi}{\partial y^2}$

finite difference pattern shown in fig. (17a)

$\sigma_y = \frac{\partial^2 \phi}{\partial x^2}$

finite difference pattern shown in fig. (17b)

$\tau_{xy} = -\frac{\partial^2 \phi}{\partial x \partial y}$

finite difference pattern shown in fig. (17c)

$\sigma_x$  Longitudinal Stresses

---

Section through 1-2

$\delta^2 \frac{\partial^2 \phi}{\partial y^2} =$

$\delta^2 \frac{\partial^2 \phi}{\partial x^2} =$

$-4\delta^2 \frac{\partial^2 \phi}{\partial x \partial y} =$

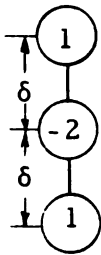


Fig. 17a.

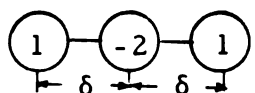


Fig. 17b.

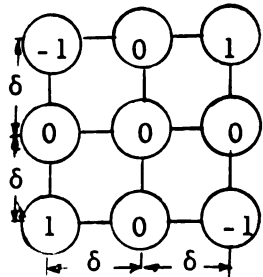


Fig. 17c.

at top	- .0606092 $\frac{F}{\delta}$
at 1	- .2424227 $\frac{F}{\delta}$
at 2	- .4242408 $\frac{F}{\delta}$
at bottom	- .6060638 $\frac{F}{\delta}$

## Section through 3-4

at top	$-.0606158 \frac{F}{\delta}$
at 3	$-.2424193 \frac{F}{\delta}$
at 4	$-.4242377 \frac{F}{\delta}$
at bottom	$-.6060702 \frac{F}{\delta}$

## Section through 5-6

at top	$-.0606438 \frac{F}{\delta}$
at 5	$-.2424043 \frac{F}{\delta}$
at 6	$-.4242247 \frac{F}{\delta}$
at bottom	$-.6060972 \frac{F}{\delta}$

## Section through 7-8

at top	$-.0607172 \frac{F}{\delta}$
at 7	$-.2423648 \frac{F}{\delta}$
at 8	$-.4241946 \frac{F}{\delta}$
at bottom	$-.6061640 \frac{F}{\delta}$

## Section 9-10

at top	$-.0608458 \frac{F}{\delta}$
at 9	$-.2422794 \frac{F}{\delta}$
at 10	$-.4241725 \frac{F}{\delta}$
at bottom	$-.6062504 \frac{F}{\delta}$

## Section 11-12

at top	$-.0608552 \frac{F}{\delta}$
at 11	$-.2421578 \frac{F}{\delta}$
at 12	$-.4244016 \frac{F}{\delta}$
at bottom	$-.6060260 \frac{F}{\delta}$

## Section through 13-14

at top	$-.0597974 \frac{F}{\delta}$
at 13	$-.2420964 \frac{F}{\delta}$
at 14	$-.4261111 \frac{F}{\delta}$
at bottom	$-.6037876 \frac{F}{\delta}$

## Section through 15-16

at top	$-.0546004 \frac{F}{\delta}$
at 15	$-.2419728 \frac{F}{\delta}$
at 16	$-.4341538 \frac{F}{\delta}$
at bottom	$-.5931464 \frac{F}{\delta}$

## Section through 17-18

at top	$-.0390094 \frac{F}{\delta}$
at 17	$-.2385204 \frac{F}{\delta}$
at 18	$-.4644451 \frac{F}{\delta}$
at bottom	$-.5550596 \frac{F}{\delta}$

## Section through 19-20

at top	$-.0104674 \frac{F}{\delta}$
at 19	$-.2134656 \frac{F}{\delta}$
at 20	$-.5573677 \frac{F}{\delta}$
at bottom	$-.447866 \frac{F}{\delta}$

$\sigma_y$  transverse Stresses

---

Location	Stresses
Edge	$-.197866 \frac{F}{\delta}$
20	$+.0453362 \frac{F}{\delta}$
18	$+.0345534 \frac{F}{\delta}$
16	$+.0137228 \frac{F}{\delta}$
14	$+.0042014 \frac{F}{\delta}$
12	$+.0010070 \frac{F}{\delta}$
10	$+.0001554 \frac{F}{\delta}$
8	$-.0000098 \frac{F}{\delta}$
6	$-.0000199 \frac{F}{\delta}$
4	$-.0000103 \frac{F}{\delta}$
2	$-.0000064 \frac{F}{\delta}$

---

Location	Stresses
Edge	$-.0104674 \frac{F}{\delta}$
19	$-.0090373 \frac{F}{\delta}$
17	$+.0064755 \frac{F}{\delta}$
15	$+.0051970 \frac{F}{\delta}$
13	$+.0020696 \frac{F}{\delta}$
11	$+.0005336 \frac{F}{\delta}$
9	$+.0000596 \frac{F}{\delta}$

7	$-.0000276 \frac{F}{\delta}$
5	$-.0000227 \frac{F}{\delta}$
3	$-.0000107 \frac{F}{\delta}$
1	$-.0000066 \frac{F}{\delta}$

---

$\tau_{xy}$  (shear stresses)

Location	Stresses
20	$-.004876175 \frac{F}{\delta}$
18	$-.005516125 \frac{F}{\delta}$
16	$-.0025985 \frac{F}{\delta}$
14	$-.0008185 \frac{F}{\delta}$
12	$-.00013105 \frac{F}{\delta}$
10	$+.00001725 \frac{F}{\delta}$
8	$+.00002525 \frac{F}{\delta}$
6	$+.000012675 \frac{F}{\delta}$
4	$+.000004325 \frac{F}{\delta}$
2	0
19	$+.03813265 \frac{F}{\delta}$
17	$+.01316005 \frac{F}{\delta}$
15	$+.0060910 \frac{F}{\delta}$

---

7	$-.0000276 \frac{F}{\delta}$
5	$-.0000227 \frac{F}{\delta}$
3	$-.0000107 \frac{F}{\delta}$
1	$-.0000066 \frac{F}{\delta}$

---

$\tau_{xy}$  (shear stresses)

Location	Stresses
20	$-.004876175 \frac{F}{\delta}$
18	$-.005516125 \frac{F}{\delta}$
16	$-.0025985 \frac{F}{\delta}$
14	$-.0008185 \frac{F}{\delta}$
12	$-.00013105 \frac{F}{\delta}$
10	$+.00001725 \frac{F}{\delta}$
8	$+.00002525 \frac{F}{\delta}$
6	$+.000012675 \frac{F}{\delta}$
4	$+.000004325 \frac{F}{\delta}$
2	0
19	$+.03813265 \frac{F}{\delta}$
17	$+.01316005 \frac{F}{\delta}$
15	$+.0060910 \frac{F}{\delta}$

---

$\tau_{xy}$  continued

Location	Stresses
13	$+ .00160995 \frac{F}{\delta}$
11	$+ .00030785 \frac{F}{\delta}$
9	$+ .00001725 \frac{F}{\delta}$
7	$- .00001915 \frac{F}{\delta}$
5	$- .000011725 \frac{F}{\delta}$
3	$- .000004175 \frac{F}{\delta}$
1	0

The variation of these stresses has been shown in the fig. no. 19.

### Principal Stresses

Since the cracks will be formed perpendicular to the maximum principal tension it will be of interest to know the magnitude and orientation of principal stresses. As it has been observed that the stresses are critical in the end block zone, the principal stresses shall be calculated for the points 16, 18, 20, 15, 17 and 19.

denoting  $\frac{F}{\delta} = p$  (pressure beneath the bearing plate)

Point 20

$$\sigma_x = -.557p$$

$$\sigma_y = +.045p$$

$$\tau_{xy} = +.004876p$$

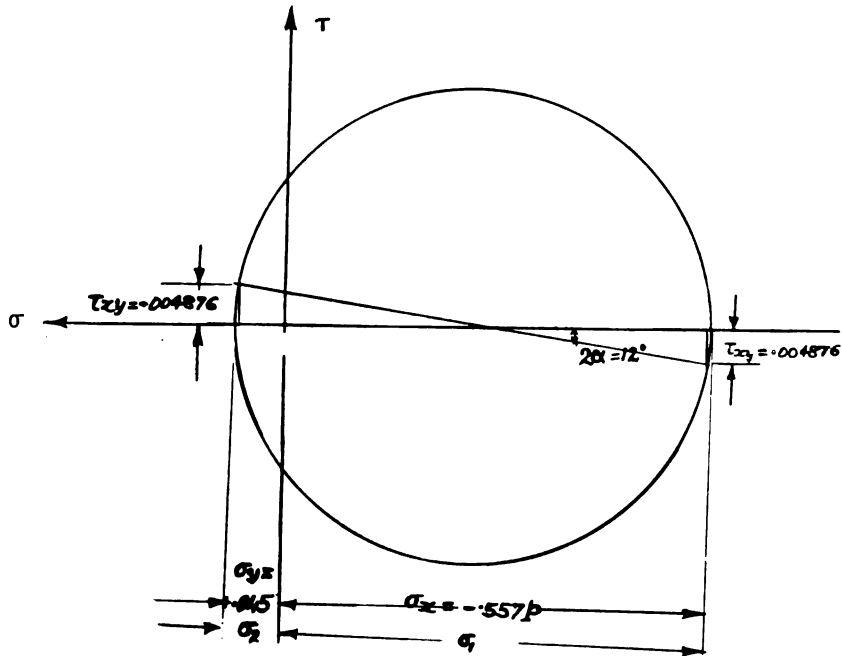


Fig. 18a. Mohr's circle for stress at point 20

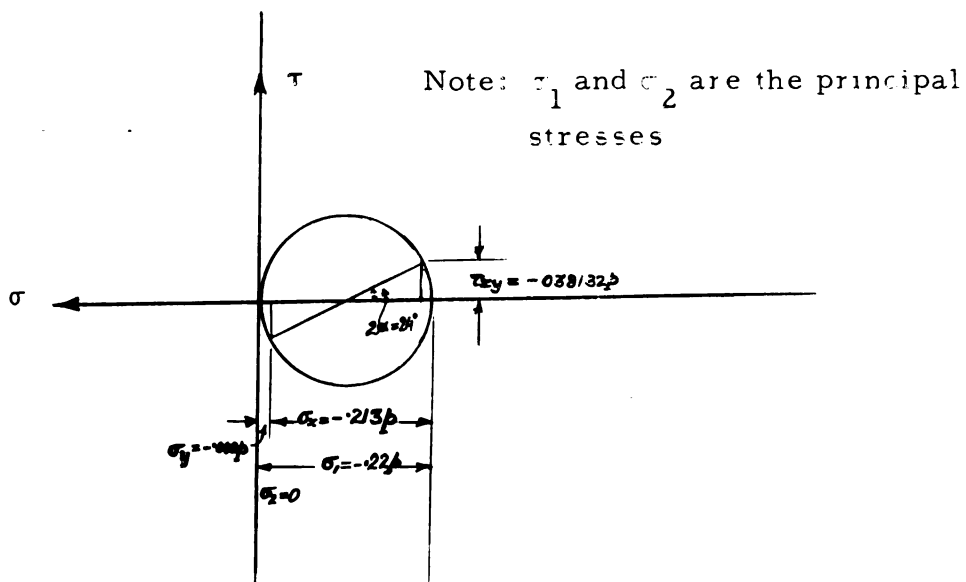


Fig. 18b Mohr's circle for stress at point 19

Point 18

$$\sigma_x = -.4644p$$

$$\sigma_y = +.03455p$$

$$\tau = -.00551p$$

Point 16

$$\sigma_x = -.434p$$

$$\sigma_y = +.0317p$$

$$\tau_{xy} = +.0025985p$$

Point 19

$$\sigma_x = -.213p$$

$$\sigma_y = +.009p$$

$$\tau_{xy} = -.03813245p$$

Point 17

$$\sigma_x = -.238p$$

$$\sigma_y = +.0064p$$

$$\tau_{xy} = -.01316005p$$

Point 15

$$\sigma_x = -.241p$$

$$\sigma_y = +.0051p$$

$$\tau_{xy} = -.0060910p$$

for each set of stresses given the Mohr's circles were drawn and the stresses determined. It is observed that since the shear stresses are very small compared to the direct stresses, the principal stresses are not very different from those of direct stresses.

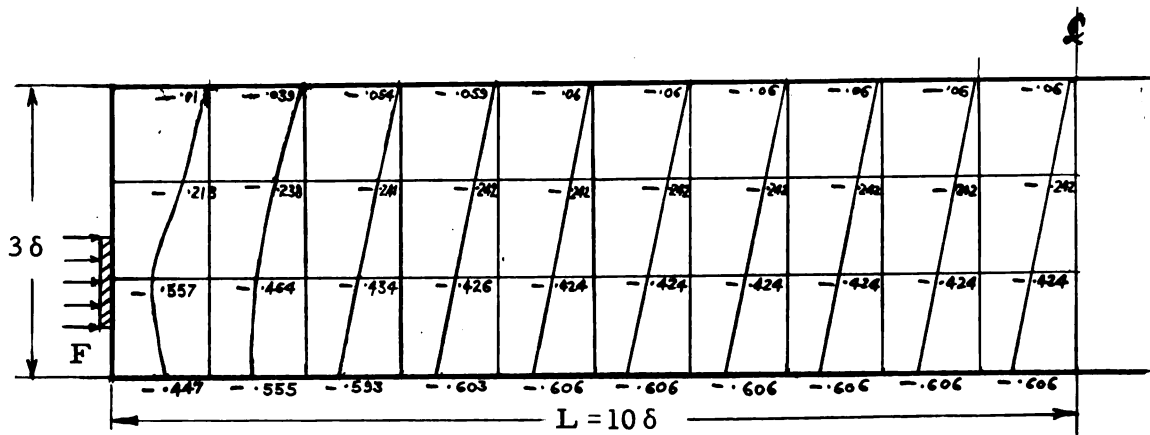


Fig. 19a. Variation of longitudinal stresses ( $\sigma_x$ ). Note: All figures have to be multiplied by  $p$  (bearing pressure) to obtain the stresses.

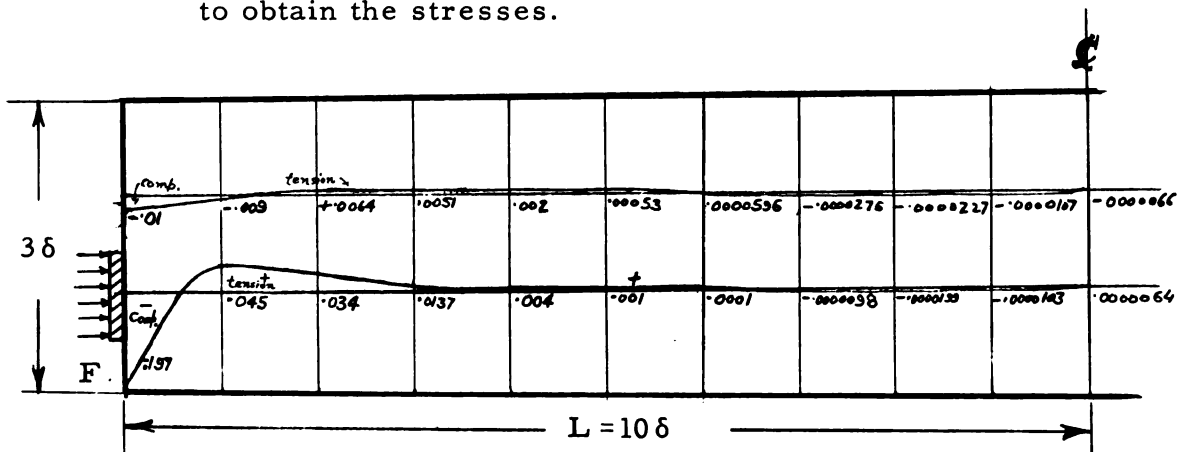


Fig. 19b. Variation of transverse stresses ( $\sigma_y$ )

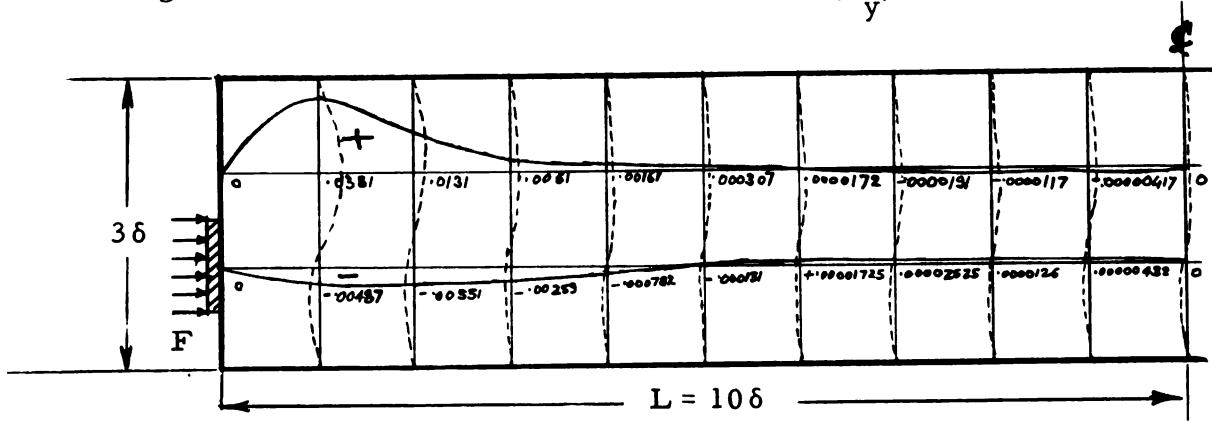


Fig. 19c. Variation of shear stresses ( $\tau_{xy}$ )

If these stresses are expressed as a ratio of the average compression over the section the following relationships are obtained:

$$\frac{F}{\delta} = p = \text{pressure beneath the bearing plate}$$

$$\frac{F}{3\delta} = p' = \text{average compressive stress over the section}$$

The maximum transverse tension

$$= .06533 \times 3p'$$

$$= .136 p'$$

this occurs at a distance of .333d, where d is the depth of the beam.

The maximum transverse compression (at the edge)

$$= .197866 \times 3p'$$

$$= .593598 p'$$

The maximum shear stress is

$$= .0381 \times 3p'$$

$$= .1143 p'$$

## V EXPERIMENTAL PROGRAM

A concrete beam 6" x 7" x 8' - 4" containing a .6000"  $\phi$  Roebling steel stranded cable ( $E_s = 24 \times 10^6$  psi) was selected.

SR-4 strain gages were used. The rosettes (AR-1) and gages were placed as shown in the fig. 20.

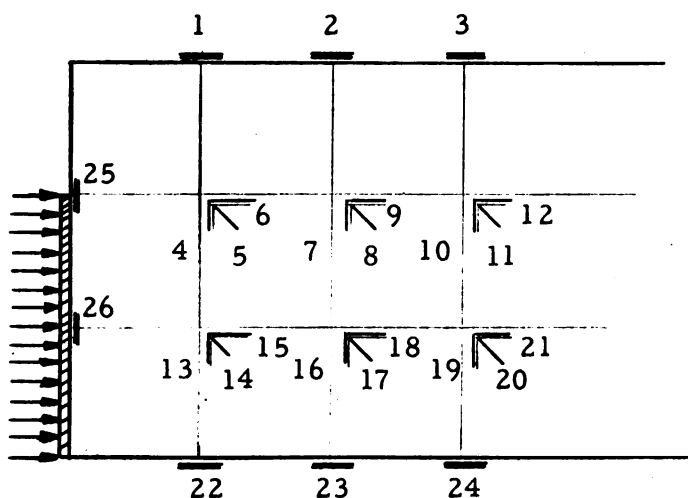


Fig. 20. Arrangement of strain gages

After the appropriate connections for the strain gages were made, the prestressing equipment consisting of hydraulic jack and cable pulling attachments (as shown in fig. 21) were fixed in position.

Initially, a tension of 2 tons was applied to the prestressing cable and initial readings of the strain indicator were taken. The load in the cable was increased to 12 tons. The strains were measured for a net prestressing force of 10 tons.

The gage readings are tabulated as given in Table 3.

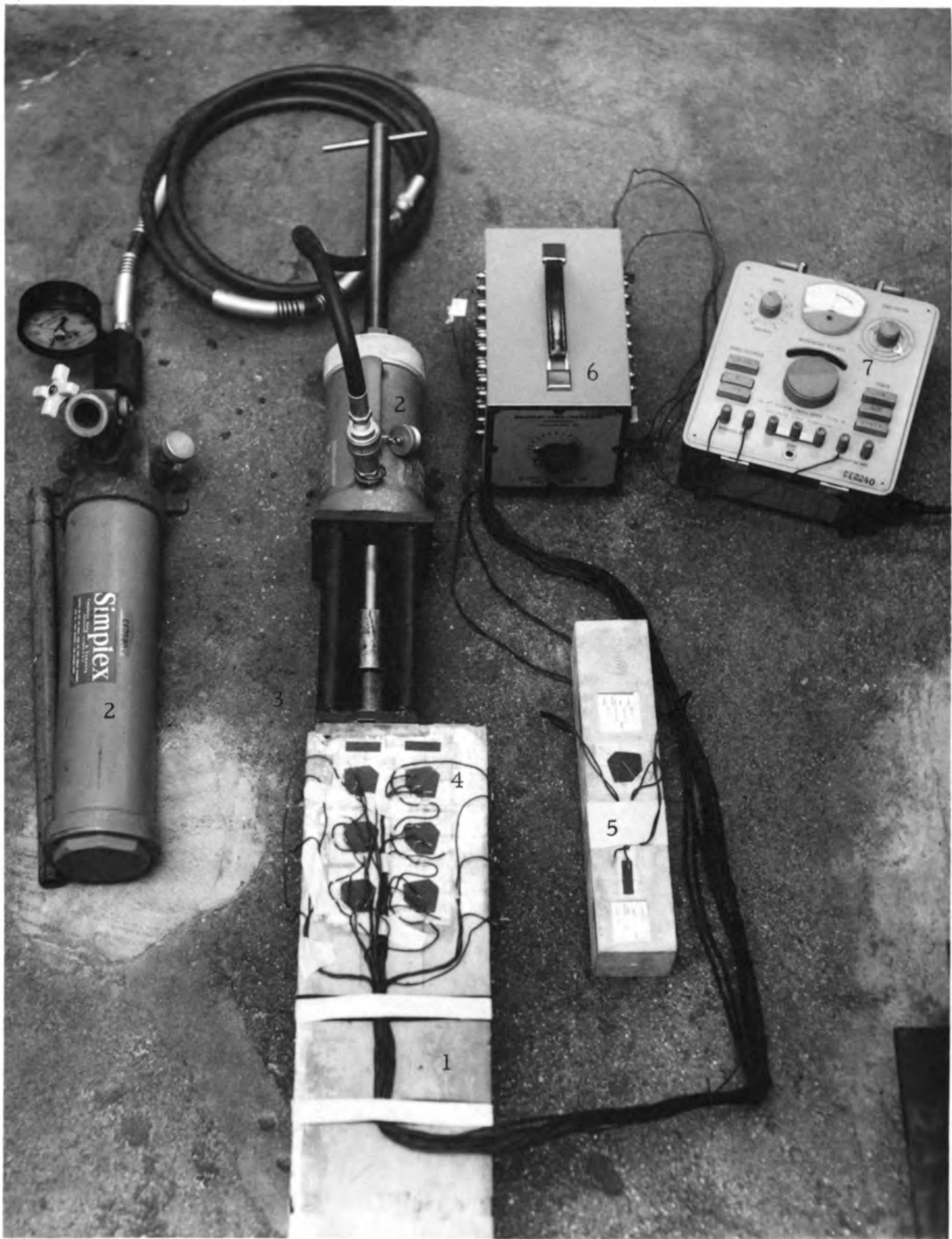


Fig. 21 Experimental Set-up

1. Beam;
2. Hydraulic Jack;
3. Cable pulling attachment;
4. Gages
5. Dummy gages;
6. Switching unit;
7. Strain Indicator.

TABLE 3

	Gage no.	Initial	Final	Strain*	Corrected* strain
Set I	4	11010	11000	-10	-7.39
	5	9415	9370	-45	-43.36
	6	12340	12225	-115	-114.98
Set II	7	9515	9530	+15	+17
	8	10787	10765	-22	-20.10
	9	11900	11812	-88	-88.34
Set III	10	11650	11672	+22	+24
	11	11332	11302	-30	-28.33
	12	11423	11335	-88	-88.27
Set IV	13	9680	9750	+70	+76.2
	14	12025	11905	-120	-116.88
	15	12660	12387	-273	-274.59
Set V	16	12015	12075	+60	+65.39
	17	9960	9840	-120	-115.65
	18	13210	12373	-237	-238.36
Set VI	19	10500	10550	+50	+54.32
	20	10082	10000	-82	-12.91
	21	10085	9895	-190	-191.13
Single gages	1	11595	11615	+20	+20
	2	10925	10930	+5	+5
	3	10715	10715	+0	+0
Single gages	22	12132	12045	+87	-87
	23	11805	11730	-155	-155
	24	10415	10185	-230	-230
Single gages	25	10940	10900	-40	-40
	26	11400	11330	-70	-70

\*Units of micro inches per inch.

Correction: if  $R_1$ ,  $R_2$ ,  $R_3$  are the indicated strains in the three directions then corrected strains  $e_1$ ,  $e_2$  and  $e_3$  are given by (fig. 22):

$$e_1 = R_1 - \frac{1}{b} R_3$$

$$e_2 = 1.02 R_2 - \frac{1}{b} (R_1 + R_3)$$

$$e_3 = R_3 - \frac{1}{b} R_1$$

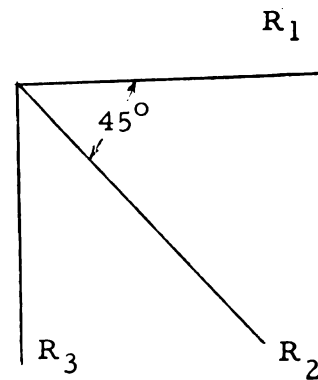


fig. 22.

where  $b$  is a constant for a particular type of gage, given by the manufacturers. In this case for the types of gages used,  $b = 44$ .

#### Example:

Taking the first set of readings corresponding to the gages 4, 5, and 6 we obtain

$$\text{Corrected strain corresponding to 4} = -10 - \frac{1}{44} (-115)$$

$$= -10 - 2.61 = -7.39$$

$$\text{Corresponding to 5} = -45 \times 1.02 + \frac{1}{44} (125)$$

$$= -46 + 2.64 = -43.36$$

$$\text{Corresponding to 6} = -115 + \frac{10}{44} = -115 + .0227$$

$$= -114.98$$

Similarly the corrections are applied for the other strain readings.

### Calculation of Stresses from Strains

Strain in any direction (fig. 23)

$$\epsilon_{\phi} = \frac{\epsilon_x + \epsilon_y}{2} + \frac{\epsilon_x - \epsilon_y}{2} \cos 2\phi + \frac{\gamma_{xy}}{2} \sin 2\phi$$

therefore

$$\begin{aligned} \epsilon_1 &= \epsilon_x \\ \epsilon_2 &= \frac{\epsilon_x + \epsilon_y}{2} + \frac{\gamma_{xy}}{2}, \quad \text{since } \phi = 45^\circ \end{aligned}$$

therefore

$$\gamma_{xy} = 2\epsilon_2 - (\epsilon_x + \epsilon_y)$$

$$\epsilon_3 = \epsilon_y$$

We also have for plane stress

$$\sigma_x = \frac{E}{1-\nu} (\epsilon_x + \nu\epsilon_y)$$

$$\sigma_y = \frac{E}{1-\nu} (\epsilon_y + \nu\epsilon_x)$$

$$\tau_{xy} = \frac{E}{2(1+\nu)} \gamma_{xy}$$

taking  $E = 4.5 \times 10^6$  psi and  $\nu = .2$  for the concrete of the beam.

$$\sigma_x = 10^6 \times 4.9 (\epsilon_x + .2\epsilon_y)$$

$$\sigma_y = 10^6 \times 4.9 (\epsilon_y + .2\epsilon_x)$$

$$\tau_{xy} = 10^6 \times 1.96 \gamma_{xy}$$

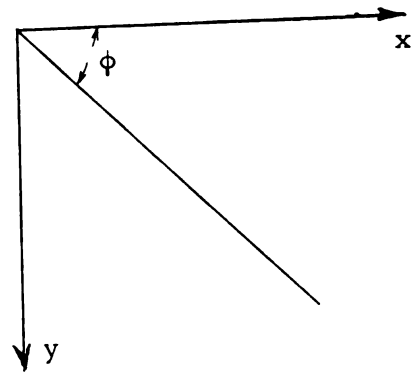


fig. 23.

Corresponding to set no. I the stresses are calculated thus:

$$\sigma_x = -4.9 (114.98 + 1.48) = -563 \text{ psi}$$

$$\sigma_y = -4.9 (7.39 + 22.996) = -142 \text{ psi}$$

$$\begin{aligned} \tau_{xy} &= 1.96 [-86.72 + (7.39 + 114.98)] \\ &= 1.96 \times 35.65 \\ &= 69.8 \text{ psi} \end{aligned}$$

Similarly stresses corresponding to the other set of strain readings can be calculated.

Table 4

Location (fig. 24a)	$\sigma_x$ psi	$\sigma_y$ psi	$\tau_{xy}$ psi
19	-563	-142	+69.8
17	-450	-3.28	+58.9
15	-418	+31.2	+33.5
20	-1270	+107	-69.4
18	-1103	+86.8	-113.5
16	-882.5	+78.4	-53
T <sub>1</sub>	+98	-	-
T <sub>2</sub>	+24.5	-	-
T <sub>3</sub>	0	-	-
B <sub>1</sub>	-426	-	-
B <sub>2</sub>	-760	-	-
B <sub>3</sub>	-1127	-	-
E <sub>1</sub>	-	-196	-
E <sub>2</sub>	-	-343	-

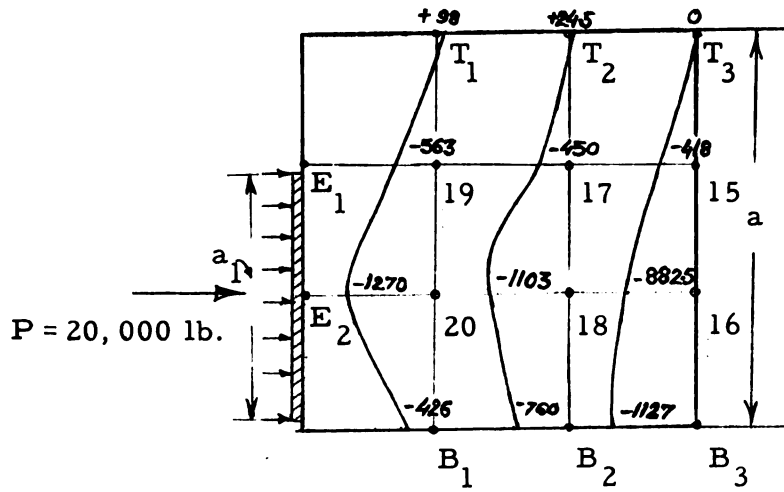


Fig. 24a. Variation of  $\sigma_x$  (experimental)

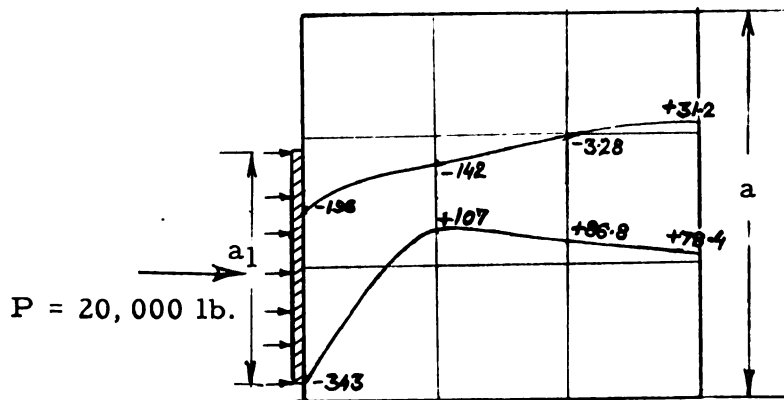


Fig. 24b. Variation of  $\sigma_y$  (experimental)

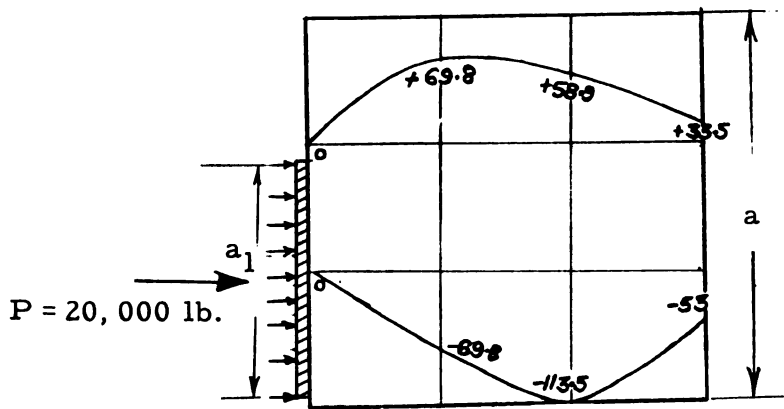


Fig. 24c. Variation of  $\tau_{xy}$  (experimental)

For the sake of comparison it is necessary to have the stresses expressed in terms of average compressive stress over the beam section.

Average stress over the cross section:

$$= \frac{20,000 \text{ psi}}{28} \quad (\text{excluding the hole})$$

$$= 714.3 \text{ psi}$$

Ratio of maximum tensile stress to the average compressive stress over the cross section:

$$\frac{107}{714.3} = .15$$

Ratio of maximum transverse compressive stress to average compressive stress over the cross section:

$$\frac{343}{714.3} = .48$$

Distance where the maximum transverse tensile stress occurs:  
.33 d from the end, where d is the depth of the beam.

Maximum shear stress expressed as a ratio of average compressive stress over the section :

$$\frac{113.5}{714.3} = .159$$

## VI DISCUSSION

The variation of the theoretical stresses  $\sigma_x$ ,  $\sigma_y$  and  $\tau_{xy}$  was in close agreement with the experimental stresses. The magnitudes of  $\sigma_x$  and  $\sigma_y$  were also in good agreement, however the theoretical values of  $\tau_{xy}$  were only 72% of the experimental values. This difference may be due to the difference in  $\frac{a_1}{a}$  ratio between the experimental and theoretical models.

A comparison is made in the following table between the analytical solution and the experimental investigation.

Description	Analytical	Experimental
1. Maximum transverse tensile stress	.136 p'	.15 p'
2. Maximum transverse compressive stress	.5935 p'	.48 p'
3. Maximum shear stress	.1143 p'	.159 p'
4. Distance where the maximum transverse tensile stress occurs	.33 d	.33 d

The differences between the theoretical and the experimental values may be attributed to the fact that the experimental beam has a hole for the prestressing cable unlike the theoretical model. Also the size of bearing plate was not the same as stipulated for the theoretical model.

The magnitude of stresses, particularly the transverse tensile stress determined by this investigation are lower than those given by Magnel, Guyon and other theories reported in the Cement Concrete Association Research Report (23), (ref. p. 30). There is also considerable variation in the magnitudes of stresses as reported in the C. C. A. research report. Therefore, it would appear that the magnitudes of stresses arrived at by this study approximates the actual stress condition.

When the end blocks were tested for failure, as reported in the C. C. A. research report, the cracks developed longitudinally up to some distance from the bearing plate. This indicated that the transverse tensile stresses are developed in the region near the bearing plate, which is confirmed by every investigation made to date.

Regarding the use of end blocks, on the basis of present investigation, it can be seen that the maximum transverse tension is  $.05 p$ , where  $p$  is the bearing pressure or  $.15 p'$ , where  $p'$  is the average compressive stress over the cross section. The temporary tensile stress permitted by the ACI code is  $3\sqrt{f'_{ci}}$ , where  $f'_{ci}$  is the compressive strength of the concrete at the time of initial prestress. The allowable tensile strength at full age is recommended as  $f'_t = \sqrt{7.5 f'_c}$ . Therefore, if the compressive strength at the time of prestressing is taken to be 4000 psi, then the ratio of tensile strength of concrete to the compressive strength is

$$\frac{\sqrt{3 f'_{ci}}}{f'_{ci}} = \frac{\sqrt{3 \times 4000}}{4000} = .0475$$

which is less than the ratio .05 p (transverse tensile stress related to the bearing pressure). As the prestressing force is increased the bearing pressure is increased and the beam should fail due to transverse tension. Since it is not economical to delay prestressing until the concrete attains its full strength, it seems that the possibility of transverse tensile failure has to be taken care of by either thickening the section in the end block zone or a combination of both.

Considering the above factors it seems that the use of end block as is conventional in the industry, in post-tensioned members is justified. However it may be dispensed with in case of pretensioned members because the prestressing force is distributed throughout the length of the member.

## VII CONCLUSIONS

As a result of the investigations carried out in this thesis it is concluded that:

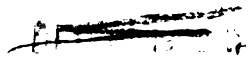
- (1) Transverse tensions of considerable magnitude are developed in the end block zone and are maximum along the plane through the center of the bearing plate.
- (2) There is transverse compression produced just beneath the bearing plate, which accounts for the resistance to lateral expansion beneath the bearing plate.
- (3) Shear stresses in the ends of the beam due to the prestressing force are small as compared to the transverse stresses.
- (4) The use of end blocks or additional transverse tensile reinforcement appears to be needed in the ends of post-tensioned beams.

## BIBLIOGRAPHY

1. Ban, S. et al. "Anchorage Zone Stress Distributions in Post-Tensioned Concrete Members," Proceedings of the World Conference on Prestressed Concrete at San Francisco, July, 1957, pp. 16
2. Bleich, F. "Der gerade stab mit Rechteckquerschnitt als ebenes Problem. Der Bauingenieur," No. 9, 1923, pp. 255-259, No. 10, 1923, pp. 304-307.
3. Bortch, R. "Die Spannungen in Walzelenkquadern," Beton und Eisen, Vol. 35, No. 4, 20, February, 1935, pp. 61-66.
4. Bortch, R. "Wälzelenke und Stelzenlager aus Eisenbeton," Beton und Eisen, Vol. 37, No. 19.5 October 1938, pp. 315-318, No. 20.20, October, 1938, pp. 328-332.
5. Carter, R. H., "Stress Distribution in the Ends of Prestressed Concrete Beams," Masters Thesis, University of Florida, 1952.
6. Christodoulides, S. P. "A Two-Dimensional Investigation of the End Anchorages of Post-Tensioned Concrete Beams," Structural Engineer, Vol. 33, No. 4, April 1955, pp. 120-133.
7. Christodoulides, S. P. "The Distribution of Stresses Around the End Anchorages of Prestressed Concrete Beams, Comparison of Results Obtained Photoclastically with Strain-Gage Measurements and Theoretical Solutions," International Association for Bridge and Structural Engineering, Vol. 16, 1956, pp. 55-70.
8. Christodoulides, S. P. "Three-Dimensional Investigation of the Stresses in the End Anchorage Blocks of a Prestressed Concrete Gantry Beam," The Structural Engineer, Vol. 35, No. 9, September, 1957, pp. 349-356.
9. Goodier, J. N. "Compression of Rectangular Blocks, and the Bending of Beams by Non-Linear Distributions of Bending Forces," Trans, A. S. M. E., (APM-54-17), Vol. 54, 1932, pp. 173-183.

10. Guyon, Y. "Stresses at Ends of Prismatic Bodies Which Are Loaded on Their Side Surface," (In French), The International Association for Bridges and Structural Engineering, Publications, Vol. 11, 1951, pp. 165-226.
11. Guyon, Y. "Prestressed Concrete," 1st edition, Concrete Publications Limited, London, 1948, pp. XV, 543. 2nd impression, John Wiley and Sons, Inc., New York, 1955, pp. 127-175.
12. Iyengar, S. R. "On a Two-Dimensional Problem in the End Block Design of Post-Tensioned Prestressed Concrete Beams," Proceedings, First Congress on Theoretical and Applied Mechanics (India), No. 6. 1-2, 1955, pp. 107-112
13. Kammüller, K. and Jeske, O. "Untersuchungen über Federgelenke aus Stahlbeton," Deutscher Ausschuss für Stahlbeton, No. 125, 1957, pp. 30.
14. Magnel, G. "Prestressed Concrete," 1st edition Concrete Publications Limited, London, 1948, pp. 63.
15. Magnel, G. "Prestressed Concrete" 3rd edition, McGraw Hill Book Co., Inc., New York, 1954, pp.
16. Magnel, G. "Design of the Ends of Prestressed Concrete Beams," Concrete and Constructional Engineering, Vol. 44, No. 5, May, 1949, pp. 141-148.
17. Mörsch, E. "Über die Berechnung der Gelenkquader," Beton und Eisen: 1924, No. 12, pp. 156-161.
18. Ramaswamy, G. S. and Goel, H. "Stresses in End Blocks of Prestressed Beams by Lattice Analogy," Proceedings of the World Conference on Prestressed Concrete at San Francisco, July, 1957, pp. 231-234.
19. Richart, F. E. "Fourth Progress Report on column tests made at the University of Illinois," (28-15), January, 1932, p. 279.
20. Sievers, H. "Die Berechnung Von Auflagerbänken und Auflagerquadern von Brückenpfeilern," Der Bauingenieur, Vol. 27, No. 6, June, 1952, pp. 209-213.

21. Sievers, H. "Über den Spannungszustand im Bereich der Ankerplatten von Spanngliedern vorgespannter Stahlbetonkonstruktionen," *Der Bauingenieur*, Vol. 31, No. 4, April, 1956, pp. 134-135.
22. Timoshenko, S. "Theory of Elasticity," 2nd edition, McGraw Hill Book Co., Inc., New York, 1951.
23. Zielinski, J. and Rowe, R. E. "An Investigation of the Stress Distribution in the Anchorage Zones of Post-Tensioned Concrete Members," *Cement and Concrete Association*, Research Report No. 9, September 1960, pp. 1-7, pp. 31-32.



ROOM USE ONLY

MICHIGAN STATE UNIVERSITY LIBRARIES



3 1293 03174 6294